Cell Reports
Article

An ER Protein Functionally Couples Neutral Lipid Metabolism on Lipid Droplets to Membrane Lipid Synthesis in the ER

Daniel F. Markgraf,[1] Robin W. Klemm,[1] Mirco Junker,[1] Hans K. Hannibal-Bach,[2] Christer S. Ejsing,[2] and Tom A. Rapoport[1,*]
[1]Department of Cell Biology, Howard Hughes Medical Institute, Harvard Medical School, Boston, MA 02115, USA
[2]Department of Biochemistry and Molecular Biology, University of Southern Denmark, 5230 Odense, Denmark
*Correspondence: tom_rapoport@hms.harvard.edu
http://dx.doi.org/10.1016/j.celrep.2013.11.046

SUMMARY

Eukaryotic cells store neutral lipids such as triacylglycerol (TAG) in lipid droplets (LDs). Here, we have addressed how LDs are functionally linked to the endoplasmic reticulum (ER). We show that, in *S. cerevisiae*, LD growth is sustained by LD-localized enzymes. When LDs grow in early stationary phase, the diacylglycerol acyl-transferase Dga1p moves from the ER to LDs and is responsible for all TAG synthesis from diacylglycerol (DAG). During LD breakdown in early exponential phase, an ER membrane protein (Ice2p) facilitates TAG utilization for membrane-lipid synthesis. Ice2p has a cytosolic domain with affinity for LDs and is required for the efficient utilization of LD-derived DAG in the ER. Ice2p breaks a futile cycle on LDs between TAG degradation and synthesis, promoting the rapid relocalization of Dga1p to the ER. Our results show that Ice2p functionally links LDs with the ER and explain how cells switch neutral lipid metabolism from storage to consumption.

INTRODUCTION

Lipid droplets (LDs) exist in virtually all cells and play a major role in human metabolic diseases, such as atherosclerosis and type 2 diabetes (Greenberg et al., 2011; Walther and Farese, 2012). LDs consist of a core of neutral lipids, comprised of triacylglycerol (TAG) and sterol esters, and a surrounding phospholipid monolayer (Fujimoto and Parton, 2011; Grillitsch et al., 2011; Leber et al., 1994; Penno et al., 2013). The size and number of LDs varies in response to changes in nutrient availability and metabolic state. LDs can expand by the esterification of diacylglycerol (DAG) with fatty acids (FAs) (Listenberger et al., 2003). Conversely, LDs can be consumed by the hydrolysis of TAGs. TAGs can be used in different ways. They can be completely hydrolyzed to generate FA and glycerol, which are ultimately used to generate ATP in the respiratory chain (Zechner et al., 2009). TAGs can also be partially hydrolyzed to generate DAG and FA, which are then used as precursors for membrane lipids (Fakas et al., 2011; Rajakumari et al., 2010; Zanghellini et al., 2008). In addition, the formation of TAG is important to avoid FA-induced lipotoxicity (Garbarino et al., 2009; Listenberger et al., 2003; Petschnigg et al., 2009).

The enzymes involved in the synthesis and degradation of neutral lipids have been identified, and some information exists on how LDs are formed. The endoplasmic reticulum (ER) appears to play a major role, as several enzymes involved in the synthesis of neutral lipids localize to the ER (Czabany et al., 2007; Natter et al., 2005). A popular model posits that LDs form by the accumulation of neutral lipids between the two leaflets of the phospholipid bilayer of the ER; the monolayer-surrounded lipid particle could either bud off into the cytoplasm or remain associated with the ER (Fujimoto and Parton, 2011; Walther and Farese, 2012). Under conditions of LD growth, some enzymes involved in the synthesis of TAG appear to be localized to LDs, suggesting that neutral lipids are not only generated in the ER (Jacquier et al., 2011; Kuerschner et al., 2008; Wilfling et al., 2013). How LDs are consumed is even less understood. One possibility is that LDs are completely autonomous: lipases sitting on LDs would hydrolyze TAGs into glycerol and FA, which in turn would be activated by acyl-coenzyme A (CoA) synthases for further metabolism. Alternatively, LD consumption may require a functional interaction between LDs and the ER. A coupling between the two organelles would not only allow the efficient conversion of DAG into membrane lipids but also prevent the accumulation of toxic levels of TAG breakdown products. A physical interaction between the two organelles has been observed in many systems, suggesting that they might indeed be functionally linked (Murphy et al., 2009).

S. cerevisiae offers a unique possibility to study the formation and consumption of LDs. LDs increase in size and number as yeast cells reach early stationary phase, and they shrink when cells are diluted into fresh medium to resume growth (Kurat et al., 2006). During LD growth, DAG is generated in the ER from phosphatidic acid (PA) by the phosphatase Pah1p (Adeyo et al., 2011; see the scheme in Figure 1A). DAG can be converted

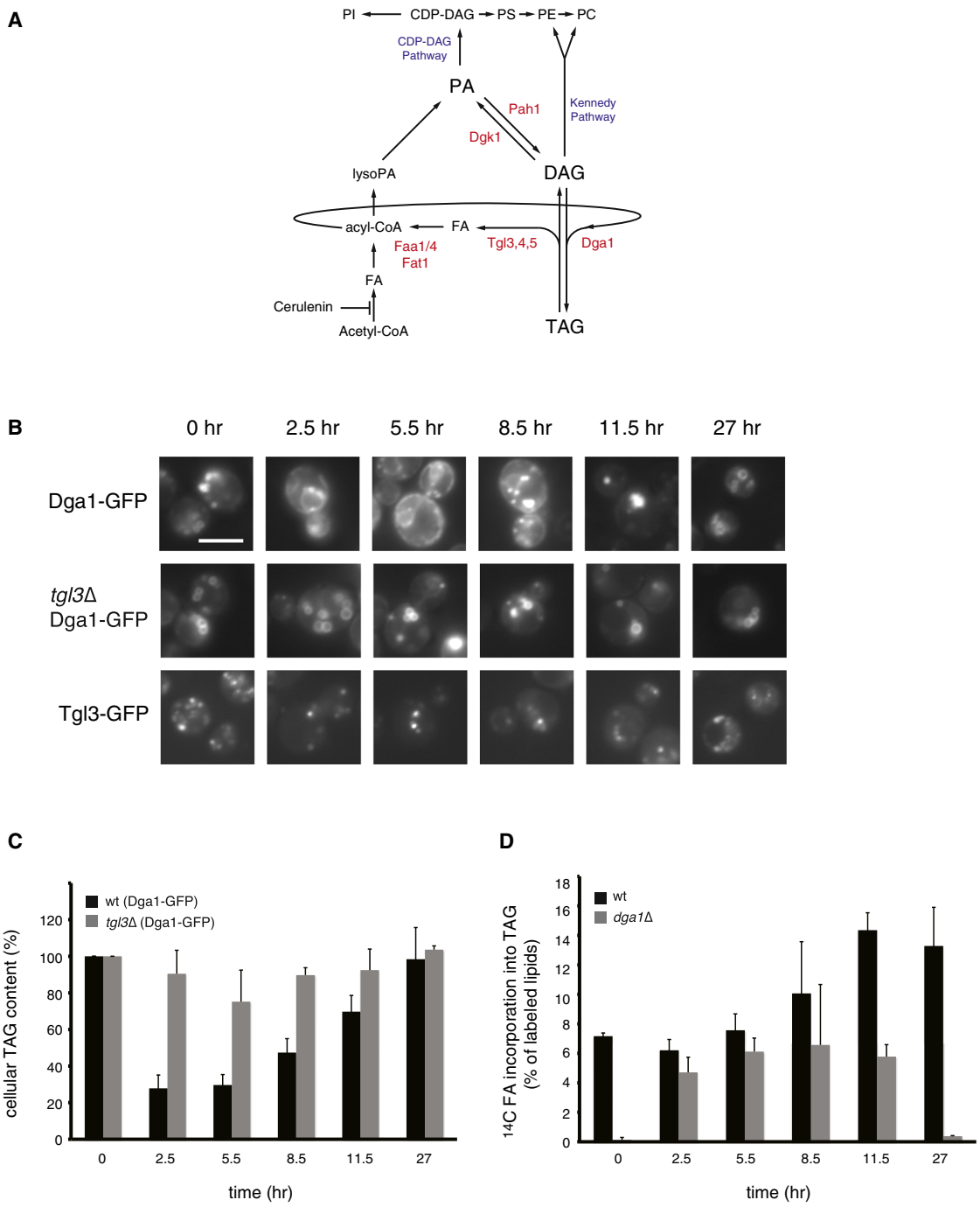

Figure 1. TAG Synthesis and Dga1p Localization on LDs

(A) Pathways connecting neutral lipid and phospholipid metabolism. Enzymes relevant to the present study are highlighted in red.

(B) Wild-type (WT) cells expressing Dga1-GFP from a plasmid or Tgl3-GFP and *tgl3*Δ mutant cells expressing Dga1-GFP from a plasmid were grown to stationary phase and then diluted into fresh medium. At the indicated time points of the growth curve (see Figure S1), cells were harvested and analyzed by fluorescence microscopy. The scale bar represents 5 μm.

(C) TAG levels were determined by TLC and iodine staining in WT (black bars) and *tgl3*Δ (gray bars) cells expressing Dga1-GFP from a plasmid. Samples were taken at the indicated time points after dilution of stationary cells into fresh medium. Data from three independent experiments are shown as mean ± SD with the TAG level at t = 0 set to 100%.

(D) The incorporation of ^{14}C-palmitic acid into TAG was determined. At the indicated time points after dilution of the cells, aliquots were taken and incubated with ^{14}C-palmitic acid for 1 hr at 30°C. ^{14}C-labeled lipids were extracted separated by TLC and quantitated by phosphorimaging and analysis by ImageJ. Labeled TAG was normalized to the total radioactivity in the chloroform-extracted fraction. Data from three independent experiments are shown as mean ± SD.

to TAG by the two diacylglycerol-acyl transferases Lro1p and Dga1p (Oelkers et al., 2002). Lro1p is an ER membrane protein and catalyzes the transfer of a fatty-acid molecule from a phospholipid to DAG (Choudhary et al., 2011; Oelkers et al., 2000). In contrast to Lro1p, Dga1p catalyzes the acyl-CoA-dependent esterification of DAG. Dga1p has two transmembrane segments, presumably forming a hairpin structure that allows localization of the enzyme to both the bilayer of the ER and the monolayer of LDs (Jacquier et al., 2011; Sorger and Daum, 2002; Stone et al., 2006). When LDs are consumed during growth resumption, lipases convert TAG into DAG and FAs, which are then used for phospholipid biosynthesis in the ER (Athenstaedt and Daum, 2003; Rajakumari et al., 2010). Three TAG lipases are known in yeast (Tgl3p, Tgl4p, and Tgl5p), with Tgl3p having the strongest effect on TAG hydrolysis in vivo (Athenstaedt and Daum, 2005; Kurat et al., 2006). Phospholipid synthesis from DAG can occur by two alternative pathways, the cytidine diphosphate (CDP)-DAG and the Kennedy pathway. In the CDP-DAG pathway, DAG is phosphorylated to PA by the kinase Dgk1p (Figure 1A; Fakas et al., 2011; Han et al., 2008). In the Kennedy pathway, ethanolamine or choline are phosphorylated and ultimately attached to DAG in the ER (Henry et al., 2012; Kuchler et al., 1986; Natter et al., 2005). Thus, during both LD growth and consumption, DAG must move between LDs and the ER, but it is unknown how the shuttling of this metabolite between the two organelles is achieved. Furthermore, although Dga1p is known to move between the ER and LDs (Jacquier et al., 2011), it is unclear whether its localization is functionally important. More generally, there is as yet no clear picture describing how LDs and the ER are functionally coupled to coordinate neutral and membrane lipid metabolism when cells switch from TAG synthesis to consumption.

Here, we have analyzed the functional connection between LDs and the ER in *S. cerevisiae*. We show that, when LDs grow during early stationary phase, Dga1p moves from the ER to LDs and is responsible for all TAG synthesis from DAG. When cells are supplied with fresh medium, LD consumption for membrane lipid synthesis is facilitated by the ER membrane protein Ice2p. Ice2p has a cytosolic domain with affinity for LDs and is necessary for the efficient channeling of DAG from LDs to membrane lipid synthesis reactions in the ER. It suppresses a futile cycle on LDs between TAG degradation and synthesis, ultimately causing Dga1p to relocalize to the ER. Our results provide a simple model for how cells switch neutral lipid metabolism from storage to consumption.

RESULTS

TAG Synthesis and Dga1p Localization on LDs

We first tested in yeast cells whether there is a correlation between TAG synthesis and Dga1p localization on LDs. Previous results showed that Dga1p moves from the ER to LDs when expression of the enzyme is induced in cells lacking all neutral lipid-synthesizing enzymes and relocalizes back to the ER during induced lipolysis (Jacquier et al., 2011). The relocalization of Dga1p does not require its de novo synthesis (Jacquier et al., 2011). We analyzed whether the localization of Dga1p would change under physiological conditions during different growth phases. We indeed found that Dga1p is localized to LDs during late exponential and stationary phases and relocalizes to the ER when cells resume growth after dilution into fresh medium (Figure 1B). The localization of Dga1p correlated with the TAG levels, as determined by thin-layer chromatography and iodine staining (Figure 1C). In stationary phase, when Dga1p is on LDs, TAG levels were high, whereas TAG decreased when Dga1p relocalized to the ER. To directly test the role of Dga1p in TAG synthesis, we measured the incorporation of ^{14}C-labeled FA into TAG by thin-layer chromatography followed by autoradiography. We found that TAG synthesis in stationary phase was almost completely abolished when Dga1p was absent (Figure 1D). In contrast, *dga1* deletion had a negligible effect on TAG synthesis during exponential growth phase. Previous studies have shown that Lro1p, the other diacylglycerol-acyl transferase, has a stronger effect on TAG synthesis during exponential phase compared to stationary phase (Oelkers et al., 2002). These results suggest that, in wild-type cells, the initial accumulation of TAGs during exponential phase occurs by Lro1p in the ER, whereas TAG synthesis during the growth of LDs in stationary phase is mainly caused by LD-localized Dga1p.

Next, we tested the localization of the major TAG lipase Tgl3p. In contrast to Dga1p, Tgl3p is localized constitutively to LDs, both in stationary and exponentially growing cells (Figure 1B). Consistent with previous studies, in the absence of Tgl3p, TAG levels were high during all growth phases (Figure 1C; Athenstaedt and Daum, 2003; Kurat et al., 2006).

Interestingly, Dga1p remained on LDs in *tgl3*Δ cells even during early exponential phase, suggesting that its relocalization to the ER in wild-type cells is caused by a decrease in TAG levels (Figure 1B). At early time points during growth resumption, when TAG levels are still high, both Dga1p and Tgl3p are present on LDs, raising the question of how net TAG degradation is initiated. One possibility is that the Dga1p substrate DAG is moved from LDs to the ER, thereby turning off TAG synthesis on LDs.

Identification of Ice2p as a Component Functionally Linking LDs and the ER

If the movement of DAG from LDs to the ER involves a protein, we reasoned that such a component should affect the delivery of DAG to Dgk1p in the CDP-DAG pathway and to enzymes in the Kennedy pathway, the two parallel pathways that use DAG for phospholipid synthesis in the ER. The effect of deletion of these enzymes on cell growth should be exacerbated if DAG channeling into the ER is reduced. We therefore searched the DRYGIN database for genes that have negative interactions with both *dgk1* and components of the Kennedy pathway. We found *ice2* to show a strong negative genetic interaction with *dgk1* (i.e., cells lacking both Dgk1p and Ice2p grow slower than cells lacking only one of these proteins) (Costanzo et al., 2010; Garbarino et al., 2009; Koh et al., 2010; Schuldiner et al., 2005; Tavassoli et al., 2013). Ice2p shows many additional genetic interactions with other lipid-metabolizing enzymes, including components of the Kennedy pathway (Table S3; Costanzo et al., 2010; Koh et al., 2010; Tavassoli et al., 2013). The genetic interaction partners of Ice2p are most similar to those of Dgk1p (Koh et al., 2010). Importantly, Ice2p also shows a positive interaction with Pah1p, the enzyme that converts PA back

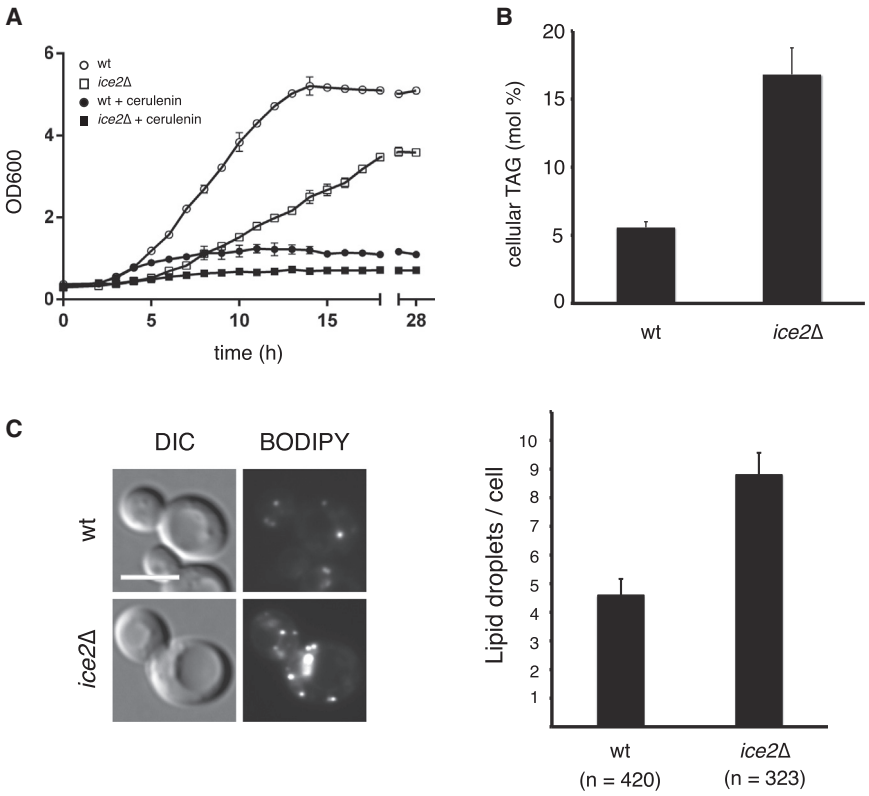

Figure 2. Ice2p Is a Component Involved in TAG Metabolism

(A) WT or *ice2*Δ mutant cells in stationary phase were diluted into fresh medium lacking or containing 10 μg/ml cerulenin, and their growth was followed by measuring the optical density (OD) at 600 nm. Shown are the mean ± SD of three independent experiments.

(B) TAG levels in WT and *ice2*Δ cells, harvested at early exponential phase, were determined after lipid extraction and analysis by mass spectrometry. Data from three independent experiments are shown as mean ± SD.

(C) LDs were stained with BODIPY 493/503 at early exponential phase and analyzed by fluorescence microscopy. Lipid droplets were quantitated using CellProfiler software (n, number of cells analyzed). The scale bar represents 5 μm. DIC, differential interference contrast.

into DAG, indicating that Ice2p might indeed be involved in providing DAG for downstream reactions. Based on these data, Ice2p could be at the functional interface between LDs and the ER and potentially be involved in DAG movement between the organelles.

Ice2p is not essential for the viability of *S. cerevisiae*, but cells lacking the protein grow significantly slower than wild-type cells. In addition, after dilution of stationary phase cells into fresh medium, an extended lag phase was observed (Figure 2A). To test whether this is caused by a defect in the utilization of LDs for phospholipid synthesis, we determined the growth of cells after dilution from stationary phase into fresh medium containing cerulenin, an inhibitor of FA synthesis (Inokoshi et al., 1994); under these conditions, cells completely rely on the degradation of TAG from LDs (Athenstaedt and Daum, 2003, 2005; Kurat et al., 2006). In the presence of cerulenin, growth of wild-type cells was not affected until up to 4 hr, whereas *ice2*Δ cells barely grew at all from the start (Figure 2A). After 4 hr, wild-type cells also stopped growing in the presence of cerulenin. These results suggest that Ice2p is required for rapid resumption of cell growth after dilution into fresh medium likely by facilitating the efficient utilization of TAG for phospholipid biosynthesis. This is consistent with a role of Ice2p in DAG channeling from LDs to the ER for phospholipid synthesis. It should be noted that a *dgk1* deletion mutant only grows slower than wild-type cells in the presence of cerulenin (Fakas et al., 2011), indicating that deletion of *ice2* has a stronger growth defect than that of *dgk1*, probably because a *dgk1* deletion can be bypassed by alternative reactions, such as the Kennedy pathway. In addition, Ice2p overexpression did not rescue the growth defect of a *dgk1* deletion mutant (data not shown). These results are consistent with the idea that Ice2p functions upstream of Dgk1p.

The absence of Ice2p led to 3-fold higher TAG levels in exponentially growing cells, determined by quantitative lipid mass spectrometry (Figure 2B). In addition, visualization of BODIPY 493/503-labeled LDs showed that *ice2*Δ cells also had a 2-fold increase in the number of LDs per cell (Figure 2C). Direct measurements of TAG breakdown showed that cells lacking Ice2p had a strong delay in TAG degradation, almost as strong as in *tgl3*Δ cells, as measured by thin-layer chromatography and iodine staining after diluting stationary cells into fresh medium in the presence (Figure 3A) or absence of cerulenin (Figure 3B). Furthermore, BODIPY 493/503-labeled LDs persisted in *ice2*Δ cells in the presence of cerulenin, whereas they were rapidly consumed in wild-type cells (Figure 3C). Taken together, these results suggest that Ice2p is required for the efficient consumption of LDs for phospholipid synthesis during growth resumption.

Ice2p Promotes TAG Consumption for Phospholipid Synthesis

Consistent with a role of Ice2p in TAG utilization for phospholipid synthesis during growth resumption, a lipid analysis by mass spectrometry showed that, even in the absence of cerulenin, *ice2*Δ cells have decreased levels of phosphatidylethanolamine (PE) and slightly reduced levels of phosphatidylcholine (PC) (Figure S2A). The decreased levels of PE are not caused by a possible effect of Ice2p on the transport of phosphatidylserine (PS) from the ER to mitochondria for decarboxylation, as no effect of *ice2* deletion was observed in an in vitro assay (Figure S2B).

To further test the function of Ice2p, we diluted stationary cells into fresh medium in the presence of cerulenin and performed quantitative lipid mass spectrometry at different time points. In

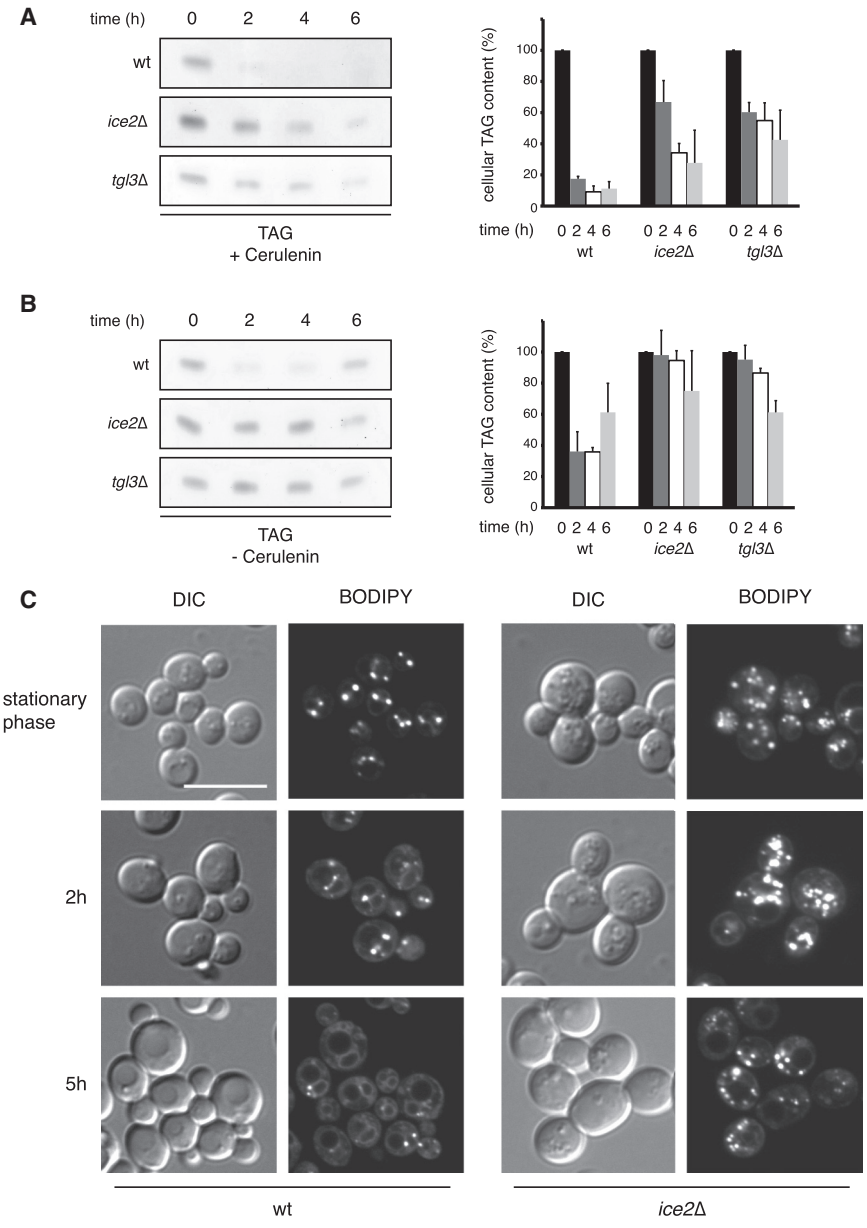

Figure 3. Ice2p Is Required for the Efficient Utilization of LDs during Growth Resumption

(A) TAG degradation was followed in WT, *ice2*Δ, and *tgl3*Δ cells after dilution of stationary phase cells into fresh medium containing 10 μg/ml cerulenin. At the indicated time points, lipids were extracted and analyzed by TLC followed by iodine staining. The graphs show quantification of three independent experiments (mean ± SD) with the TAG level at t = 0 set to 100%.

(B) As in (A), but stationary cells were diluted into fresh medium without cerulenin.

(C) The consumption of LDs in WT and *ice2*Δ cells after dilution from stationary phase into fresh medium containing 10 μg/ml cerulenin was followed by BODIPY 493/503 staining and fluorescence microscopy. The scale bar represents 10 μm.

wild-type cells, TAG levels decreased rapidly, whereas PA, PE, and PC increased (Figures 4A and 4C–4E). DAG decreased with some delay, as expected from it being an intermediate metabolite (Figure 4B). In *ice2*Δ cells, TAG degradation was significantly delayed and DAG levels remained high, particularly at later time points (Figures 4A and 4B). No or little increase in phospholipid levels was observed (Figures 4C–4E). These data show that, in *ice2*Δ cells, LD-derived DAG cannot be utilized by the PA-generating enzyme Dgk1p in the ER, ultimately affecting the synthesis of PA, PE, and PC. No major differences in the levels of PS and phosphatidylinositol between wild-type and *ice2*Δ cells were observed during growth resumption (Figure S3A). Altogether, these results support the idea that Ice2p is required for the efficient channeling of DAG from LDs to the ER for phospholipid synthesis. It should be noted that the growth defect of *ice2*Δ cells could not be rescued with 1 mM ethanolamine or choline (data not shown), compounds that would stimulate phospholipid synthesis via the Kennedy pathway if DAG were available in the ER. These results support the notion that Ice2p is required for the efficient channeling of DAG from LDs to the ER for phospholipid synthesis and acts upstream of Dgk1p.

Ice2p Facilitates Metabolic Channeling of DAG from LDs to the ER

If Ice2p was required for channeling of DAG from LDs to the ER during growth resumption, then one would expect that, in the absence of Ice2p, DAG would be generated by lipases such as Tgl3p, but would not be available for the Dgk1p enzyme in the ER. This would be expected to lead to a futile cycle, in which TAG is continuously broken down and resynthesized from DAG by Dga1p (Figure 1A).

This assumption is supported by experiments in which we radiolabeled TAG and studied its conversion into DAG during growth resumption in the presence of cerulenin. In agreement with the mass spectrometry results, *ice2* deletion led to delayed TAG degradation and increased DAG levels (Figures S3B and S3C). Importantly, the simultaneous absence of both Ice2p and Dga1p did not change TAG degradation but led to even higher DAG levels, consistent with a disrupted futile cycle. As expected, the absence of Tgl3p impaired TAG hydrolysis and resulted in rapid consumption of DAG (Figures S3B and S3C).

To directly test the resynthesis of TAG from DAG, we added ^{14}C-labeled palmitic acid to cells immediately after dilution from stationary phase into fresh medium containing cerulenin. The incorporation of labeled FA into TAG was followed by

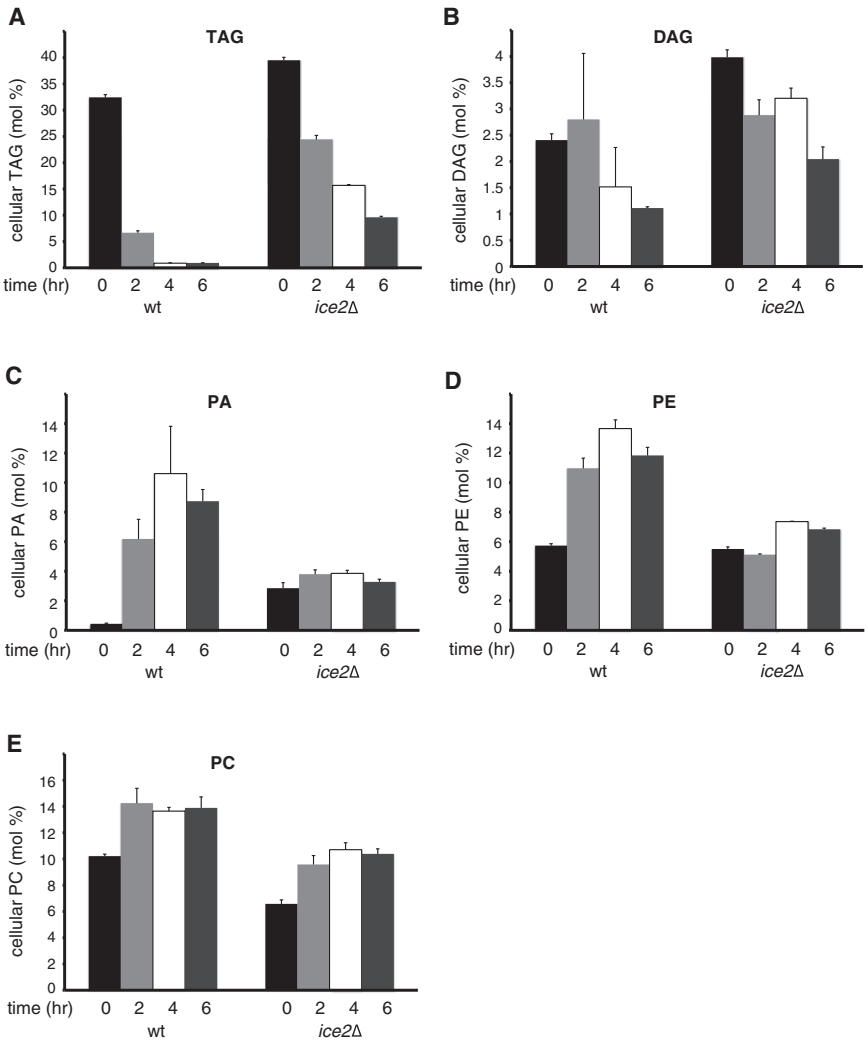

Figure 4. Ice2p Promotes TAG Consumption for Phospholipid Synthesis

The lipid composition of WT and *ice2*Δ cells was analyzed at different time points after dilution from stationary phase into fresh medium containing 10 μg/ml cerulenin. The indicated lipid species were analyzed by quantitative mass spectrometry. Data from two independent experiments were analyzed in duplicates and are shown as mean ± SD.

thin-layer chromatography and autoradiography. Wild-type cells showed some weak, transient TAG labeling, whereas *ice2*Δ cells synthesized TAG over an extended period (Figure 5A). Cells lacking the major lipase Tgl3p showed very little TAG synthesis. When ^{14}C-labeled palmitic acid was added 2 hr after dilution into fresh medium, wild-type cells did not incorporate any label into TAG, whereas TAG synthesis was still observed in *ice2*Δ cells (Figure 5B). In wild-type cells diluted into fresh medium containing cerulenin, the esterification of DAG with ^{14}C-labeled palmitic acid was completely dependent on Dga1p (Figure S4A), confirming that this is the major enzyme required for the resynthesis of TAG on LDs (see also Figure 1D). Cells lacking both Ice2p and Dga1p still showed some re-esterification (Figure S4A). Given that Lro1p can localize close to LDs in stationary phase (Wang and Lee, 2012), we assume that it partially replaces Dga1p under these conditions, preventing the accumulation of toxic DAG levels. Similar results were obtained when ^{14}C-labeled oleic acid was used instead of ^{14}C-labeled palmitic acid (Figure S4B). Taken together, these results provide strong support for the idea that, in *ice2*Δ cells, there is continuous re-esterification of DAG generated by hydrolysis from TAG; in the absence of TAG hydrolysis (in *tgl3*Δ cells), less DAG is generated that could serve as a substrate for resynthesis of TAG. Consistent with this model, Dga1p stayed on LDs in *ice2*Δ cells when cells were diluted into fresh medium containing cerulenin, in contrast to the situation in wild-type cells, where it moved to the ER (Figure 5C). Tgl3p also stayed on LDs in *ice2*Δ cells (Figure 5D). Thus, in the absence of Ice2p, there is a futile cycle on LDs in which TAG is broken down by Tgl3p and resynthesized by Dga1p. The activation of the FA generated by Tgl3p can occur by the acyl-CoA synthetases Faa1p, Faa4p, and Fat1p, which all have been reported to localize to LDs (Athenstaedt et al., 1999; Natter et al., 2005).

Ice2p Links LDs to the ER for Efficient DAG Shuttling

If Ice2p has a role in channeling DAG from LDs to the ER, one would expect that it localizes to the interface between the two organelles. In agreement with previous results (Estrada de Martin et al., 2005), GFP-tagged Ice2p (Ice2-GFP) localized to the ER in exponentially growing cells (Figure 6A; the GFP-tagged protein is functional, see Figure S5A). However, in stationary phase, Ice2-GFP accumulated in punctate structures adjacent to LDs labeled with red flourescent protein (RFP)-tagged Erg6p (Erg6-RFP) (Figures 6A and 6B). When stationary cells were diluted into fresh medium, Ice2-GFP rapidly relocalized from the LD-proximal sites back to the ER (Figure 6C). Relocalization of Ice2-GFP occurred within 30 min after dilution, preceding the relocalization of Dga1p to the ER (Figure S5B). Interestingly, relocalization of Ice2-GFP to the ER was also observed in *tgl3*Δ cells (Figure 6C) where Dga1p stayed on LDs (see Figure 1B), indicating that Ice2p localization is not determined by TAG levels in LDs. Overexpressed Ice2-GFP localized to the ER, but when oleate was added to generate large LDs, it was also found in sheet structures around LDs (Figure S5C).

The localization of Ice2p to LD-proximal sites suggested that the protein might have a segment that interacts with LDs. Ice2p

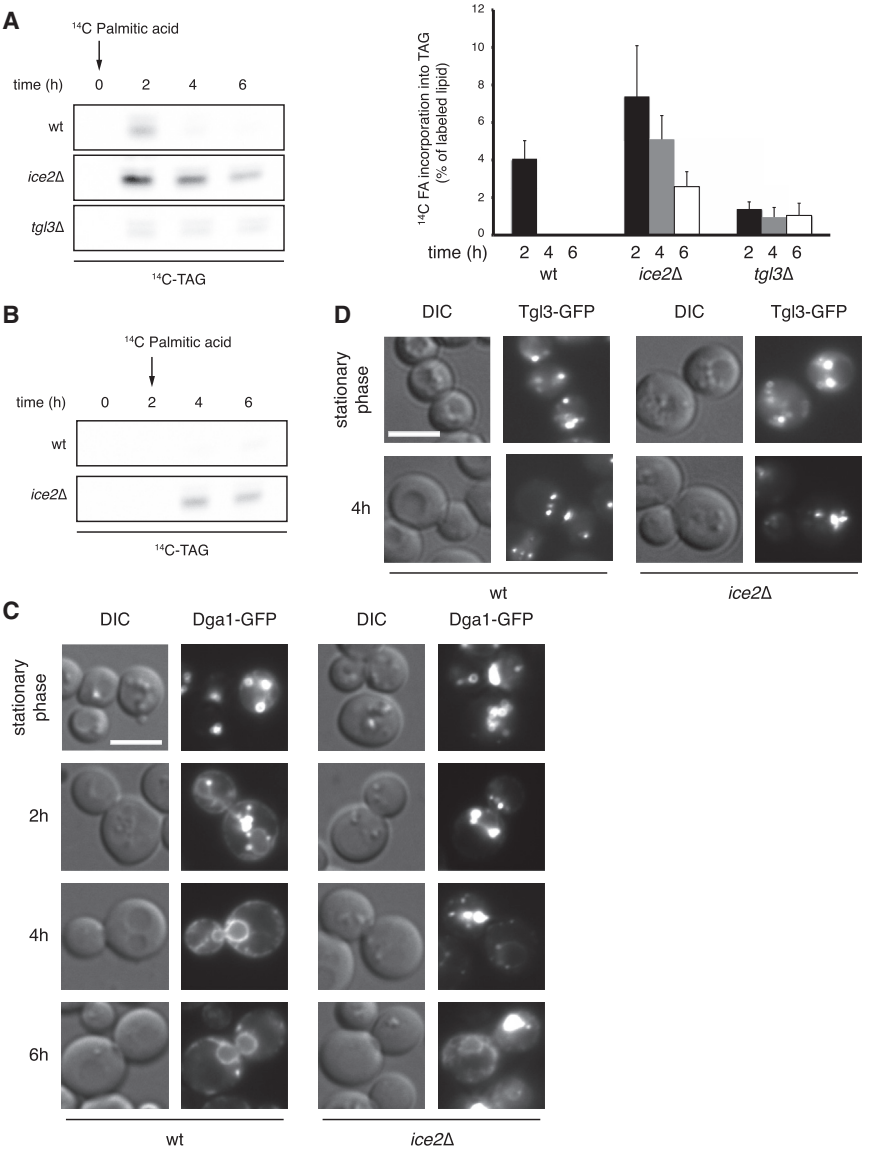

Figure 5. Ice2p Suppresses a Futile Cycle between TAG and DAG on LDs

(A) The resynthesis of TAG in WT, *ice2*Δ, and *tgl3*Δ cells was analyzed by adding ^{14}C-palmitic acid to cells immediately after their dilution from stationary phase into fresh medium containing 10 μg/ml cerulenin. At the indicated time points aliquots were taken, lipids were extracted and analyzed by TLC. Labeled TAG on the TLC plate (left panel) was quantitated by phosphorimaging (right panel). The data were normalized to the total radioactivity in the chloroform-extracted fraction and are presented as mean ± SD of four independent experiments.

(B) As in (A), but the ^{14}C-palmitic acid was added 2 hr after dilution of WT or *ice2*Δ cells.

(C) The localization of Dga1-GFP, expressed from a plasmid, was followed by fluorescence microscopy in WT and *ice2*Δ cells after dilution from stationary phase into fresh medium containing 10 μg/ml cerulenin.

(D) As in (C), but the localization of Tgl3-GFP was determined in stationary phase and 4 hr after dilution. The scale bars represent 5 μm.

is a predicted multispanning membrane protein with only one sizable hydrophilic domain (TMHMM server v 2.0; see scheme in Figure 7A; Estrada de Martin et al., 2005). This domain is predicted to be on the cytoplasmic side of the ER membrane (Ice2(cyt)) and would thus be a candidate to interact with LDs. Indeed, it is predicted to contain four amphipathic helices (Jpred, PSIPRED v3.3, PredictProtein, and Robetta; Figure 7B), a common LD-targeting motif (Walther and Farese, 2012). To test whether this domain interacts with LDs, we expressed this segment as a GFP fusion (Ice2(cyt)-GFP) in yeast cells together with the LD marker Erg6-RFP. Both proteins colocalized (Figure 7C), indicating that the cytoplasmic domain of Ice2p indeed has an affinity for LDs. Occasionally, some ER staining was also seen (Figure S6A). When cells were incubated with oleate to generate large LDs, Ice2(cyt)-GFP localized exclusively to LDs (Figure 7C).

To further ascertain that the cytoplasmic domain of Ice2p interacts with LDs, we expressed an RFP fusion (RFP-Ice2(cyt)) in mammalian COS7 cells. The protein localized to the surface of LDs stained with BODIPY 493/503; no colocalization with the ER marker calreticulin was observed (Figure 7D). Given that Ice2p has no obvious homolog in mammalian cells, these data suggest that the cytoplasmic domain interacts with the lipids in LDs, rather than with a protein.

Finally, the overexpression of a mutant of Ice2p lacking the cytoplasmic domain only partially rescued the growth phenotype of an *ice2*Δ strain (Figure S6C). The protein localized to the ER (Figure S6B) but did not accelerate TAG breakdown or prevent the accumulation of DAG (Figures S6D and S6E) in *ice2*Δ cells. Taken together, these results support the idea that the ER membrane protein Ice2p has a cytoplasmic domain that interacts with LDs and is required for its function.

DISCUSSION

We show that, during LD growth in late exponential and stationary phase, all TAG synthesis occurs by Dga1p on LDs. Net TAG consumption during growth resumption is achieved by lipases, such as Tgl3p, that always stay on LDs. However, because Dga1p is also initially localized to LDs during growth resumption, there must be a mechanism that suppresses a futile cycle between DAG and TAG to allow net TAG degradation. We show that, during early phases of TAG breakdown, futile cycling is inhibited by Ice2p, a multispanning membrane protein of the ER.

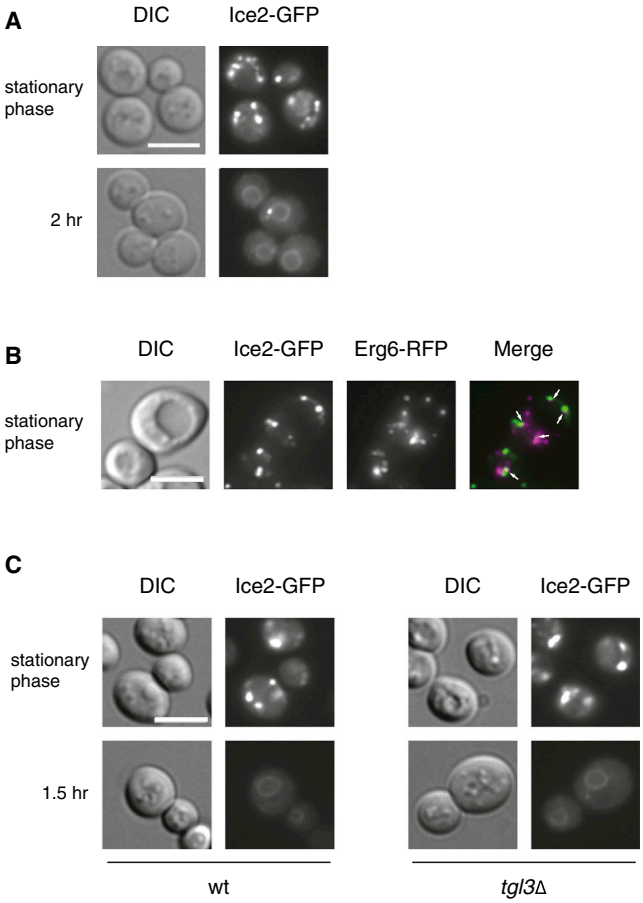

Figure 6. Growth-Phase-Dependent Localization of Ice2p

(A) The localization of Ice2-GFP was analyzed by fluorescence microscopy at stationary phase and 2 hr after dilution into fresh medium.

(B) The localization of Ice2-GFP was analyzed by fluorescence microscopy in stationary phase cells expressing Erg6-RFP. Six optical sections along the z-axis were collected with a step size of 0.5 μm. A maximum projection is shown. Arrows indicate areas of contact between Ice2-GFP- and Erg6-RFP-labeled LDs.

(C) The localization of Ice2-GFP was analyzed in wild-type (WT) and *tgl3*Δ cells in stationary phase and 1.5 hr after dilution into fresh medium containing 10 μg/ml cerulenin. The scale bars represent 5 μm.

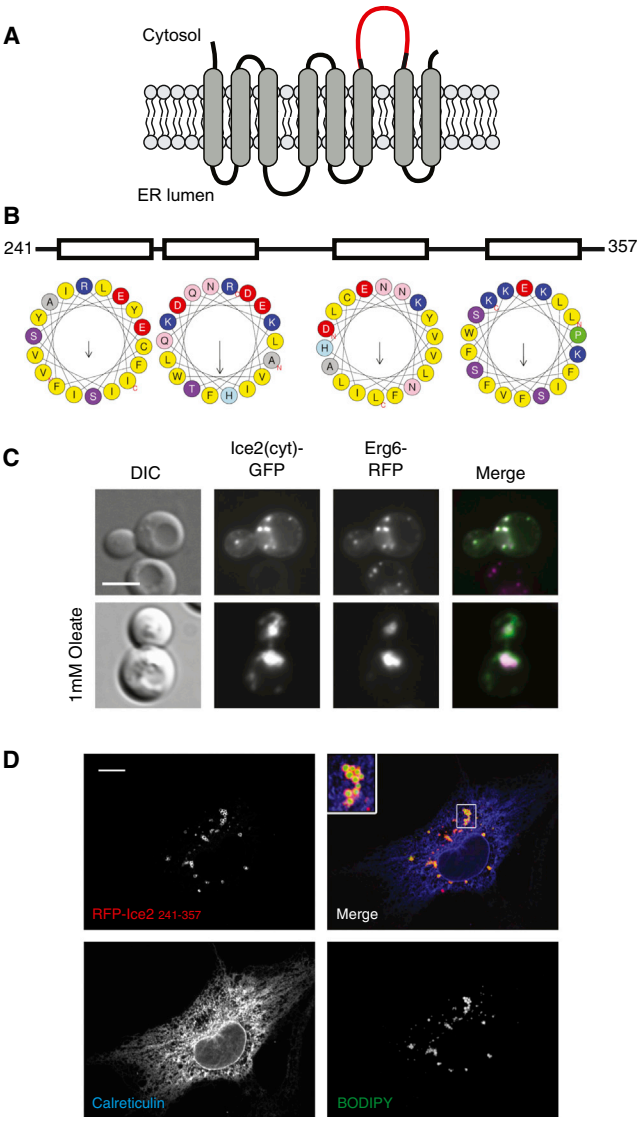

Figure 7. A Cytoplasmic Domain of Ice2p Binds to Lipid Droplets

(A) Predicted topology of Ice2p. The largest cytoplasmic loop (amino acids 241–357) is highlighted.

(B) Predicted secondary structure of the cytoplasmic loop of Ice2p. Helical wheel representations of predicted helices were generated using the program HeliQuest (http://heliquest.ipmc.cnrs.fr/).

(C) The localization of a fusion between the cytosolic loop and GFP (Ice2(cyt)-GFP), expressed from a plasmid, was analyzed by fluorescence microscopy in exponentially growing cells. The cells also expressed Erg6-RFP as a marker for LDs. Lower panel shows cells grown in the presence of 1 mM oleate. The scale bar represents 5 μm.

(D) The localization of RFP-Ice2(cyt) was analyzed by fluorescence microscopy in COS7 cells. The cells were also stained with BODIPY 493/503 for LDs and for the ER marker calreticulin by immunofluorescence microscopy. The scale bar represents 10 μm.

Ice2p facilitates the channeling of DAG from LDs to the ER, a process that shifts the metabolism to efficient phospholipid synthesis and prevents the accumulation of toxic DAG levels. The Ice2p-mediated regulation of a futile cycle on LDs thus presents an important regulatory mechanism in lipid homeostasis. Ice2p has a cytoplasmic loop that targets it to LDs. In a second phase, when TAG levels are sufficiently reduced, Dga1p is moved from LDs to the ER, terminating TAG synthesis on LDs. These results explain how yeast cells can switch from TAG synthesis to consumption.

In *S. cerevisiae*, essentially all LDs appear to be in close proximity of the ER (Szymanski et al., 2007; Wolinski et al., 2011). Fluorescence recovery after photobleaching experiments suggest that LDs may be associated with the ER through phospholipids (Jacquier et al., 2011). LDs remain close to the ER in *ice2*Δ cells (data not shown), indicating that Ice2p is not required for the association of the two organelles. Ice2p function does not seem to be restricted to the interface between LDs and the ER. In fact, during growth resumption, Ice2p relocalizes much faster from an

LD-associated ER domain to the bulk ER than TAG levels decrease (Figure S5B). Its steady-state distribution during different growth phases thus reflects the primary site of DAG utilization; it localizes to the proximity of LDs during DAG-to-TAG conversion in LDs and to the bulk ER during DAG utilization by phospholipid-synthesizing enzymes. One possible model for how Ice2p might function is that it shuttles DAG directly between the two organelles. If Ice2p is required for the shuttling of DAG, one would have to assume that there is a barrier between LDs and the ER that prevents the free diffusion of the metabolite, despite the fact that the two organelles are contiguous. In principle, Ice2p could also be an activator of Dgk1p, but this would not explain the genetic interaction between the two proteins.

We consider it unlikely that Ice2p is required for metabolic channeling of FA, the other breakdown product of TAG. In contrast to DAG, FA utilization may not require physical contact between LDs and the ER. FAs could be efficiently activated on LDs by acyl-CoA synthetases (Athenstaedt et al., 1999; Natter et al., 2005) and subsequently be moved by acyl-CoA-binding proteins through the cytosol to the ER, mitochondria, or peroxisomes (Rasmussen et al., 1994).

Our results lead to a simple model for how yeast cells can switch from TAG synthesis to consumption during different growth phases. During late exponential and early stationary phase, Pah1p generates DAG and Dga1p moves to LDs, where it converts DAG into TAG. LD-localized TAG synthesis by enzymes that move from the ER to growing LDs has also been observed in mammalian cells (Wilfling et al., 2013). In contrast, the ER-localized acyl transferase Lro1p, the other major enzyme converting DAG into TAG in yeast, appears to have its major role in TAG synthesis during exponential growth (Oelkers et al., 2002). Thus, in wild-type cells, it may generate the first TAG molecules when LDs are formed de novo, whereas Dga1p would move into the LDs and take over TAG synthesis only when the LDs have reached a sufficient size. The ER-localized diacylglycerol acyltransferase 1 (DGAT-1) enzyme in mammalian cells can also only generate small LDs (Wilfling et al., 2013). However, it should be noted that, in yeast cells lacking Lro1p, Dga1p alone is sufficient to generate LDs (Sandager et al., 2002), and it is possible that Lro1p can partially replace Dga1p in *ice2*Δ *dga1*Δ cells to recycle DAG to TAG (Figure S4A).

When cells exit stationary phase and resume growth, TAG is hydrolyzed to DAG and FA by lipases such as Tgl3p and DAG is channeled back into the ER by Ice2p and utilized by Dgk1p and the Kennedy pathway for phospholipid synthesis. When TAG levels are sufficiently reduced, Dga1p is moved from LDs to the ER, terminating TAG synthesis on LDs. Previous results indicated that regulated lipase activity is critical for efficient growth resumption (Kurat et al., 2009), but our experiments now indicate that there is an important step in the ER succeeding actual TAG hydrolysis. Recent results in mammalian cells suggest that lipases can degrade TAG to 1,3-DAG (Eichmann et al., 2012), which cannot directly be used for phospholipid synthesis. However, 1,3-DAG is the preferred substrate for DGAT-2, the homolog of yeast Dga1p, suggesting that a futile cycle between TAG and DAG occurs in mammals as well (Eichmann et al., 2012). We have not been able to detect 1,3-DAG in our TAG degradation experiments in yeast (data not shown), so it is possible that 1,2-DAG is used for both TAG and phospholipid synthesis. In both mammals and yeast, it is also conceivable that isomerases exist, which interconvert the DAG species. Regardless of the specificity of the lipases, our results indicate that the switch between net TAG synthesis and hydrolysis would be determined by three factors: (1) generation or consumption of DAG in the ER, (2) Ice2p-mediated metabolic channeling of DAG from LDs to the ER, and (3) movement of Dga1p between the ER and LDs.

How does Dga1p move between the ER and LDs? We assume that it behaves similar to its mammalian homolog, DGAT-2, which has an N-terminal hydrophobic domain, but no hydrophilic segment on the luminal side of the ER membrane, allowing it to sit not only in the lipid bilayer of the ER but also in the monolayer of LDs (Stone et al., 2006; Wilfling et al., 2013). Our results support the idea that Dga1p partitions into LDs simply because of its interaction with the hydrophobic core of LDs or the surrounding monolayer. Such a model would also explain why several other proteins, including Erg6p and Faa4p in yeast and DGAT-2, CTP-phosphocholine cytidylyltransferase, and PAT proteins in mammals, associate with expanding LDs, despite the fact that they do not share sequence similarity (Athenstaedt et al., 1999; Bickel et al., 2009; Jacquier et al., 2011; Krahmer et al., 2011; Wilfling et al., 2013). Targeting of Ice2p to LD-proximal ER domains is mediated by a cytosolic loop. This domain is predicted to contain four amphipathic helices. A similar motif is found in the LD-binding protein TIP47 and the neutral lipid-interacting apolipoprotein E (apo E) (Walther and Farese, 2012). Structures for these proteins showed that the amphipathic helices are arranged in a four-helix bundle, which is stabilized by a hydrophobic core (Hickenbottom et al., 2004; Wilson et al., 1991). Opening of the four-helix bundle and exposure of hydrophobic sequences allows apo E to bind to lipid surfaces (Brasaemle, 2007; Raussens et al., 1998). A similar mechanism is discussed for TIP47, which would allow its movement from the cytosol to nascent lipid droplets (Bulankina et al., 2009). It is thus tempting to speculate that the cytosolic domain of Ice2p is also arranged in a four-helix bundle and, upon rearrangement, would expose hydrophobic surfaces for interaction with LDs. Interestingly, the cytoplasmic domain of Ice2p localized to LDs even in exponentially growing cells (Figure 7C), when the full-length Ice2p was found in the ER (Figures 6A and 6C). This result would be consistent with the possibility that Ice2p undergoes a conformational change when cells enter stationary phase, exposing the cytosolic domain for interaction with LDs.

DAG channeling between LDs and the ER might also occur in higher eukaryotes, but its importance might differ between cell types. In adipocytes, TAGs serve primarily as an energy source and are therefore further hydrolyzed to monoacylglycerol and glycerol (Duncan et al., 2007; Zechner et al., 2009). In contrast, in the liver of mammals, lipolytic products of TAG are precursors for lipoprotein particle synthesis in the ER (Lankester et al., 1998; Wiggins and Gibbons, 1992; Yang et al., 1995). Thus, it is possible that similar pathways as in *S. cerevisiae* may exist, albeit with components that have no obvious sequence similarity.

Ice2p had previously been implicated in ER inheritance from the mother to the daughter cell (Estrada de Martin et al., 2005).

The effect of *ice2* deletion on ER morphology is only observed at early stages of bud formation and is relatively weak. It can easily be explained by our observation that Ice2p plays a role in the conversion of TAG into phospholipids. Consistent with this explanation, cells lacking both Ice2p and Scs2p, a protein that binds the transcriptional repressor Opi1p to regulate phospholipid-synthesizing enzymes (Henry et al., 2012; Kagiwada et al., 1998; Loewen and Levine, 2005), have increased defects in cortical ER morphology (Loewen et al., 2007; Tavassoli et al., 2013). Ice2p has also been described as a protein required for optimal growth when Zn^{2+} ions are limiting (North et al., 2012). Although in our experiments Zn^{2+} is not limiting (data not shown), it is easy to see why the deletion of Ice2p would exacerbate the effect of low Zn^{2+} concentrations. Deletion of *ice2* leads to lower phospholipid levels, and low Zn^{2+} levels also result in lowered PS and PE levels, caused by the activation of phosphatidylinositol synthetase (Pis1p) and of the PA hydrolase Pah1p through relief of Zn^{2+}-dependent transcription repression (Han et al., 2005; Henry et al., 2012; Soto-Cardalda et al., 2012). Taken together, the identification of the function of Ice2p in DAG channeling from LDs to the ER explains a number of previous seemingly unrelated and puzzling observations.

EXPERIMENTAL PROCEDURES

Yeast Strains and Plasmids

Tagging of proteins and gene deletions were performed by standard PCR-based homologous recombination (Longtine et al., 1998). Strains used in this study are isogenic to BY4741 (Mat a ura3Δ his3Δ1 leu2Δ0 met15Δ0) and are listed in Table S1. Plasmids used in this study are listed in Table S2 and described in the Supplemental Information.

Growth Conditions

Cells were grown at 30°C in synthetic complete (SC) medium. SC medium contained 1.7 g/l yeast nitrogen base without ammonium sulfate (MP Biomedical), 5 g/l ammonium sulfate (Sigma-Aldrich), and 20 g/l glucose and was supplemented with the required amino acid mixtures (Complete Supplement Mixture [CSM] 0.79 g/l; CSM-leucine 0.69 g/l; Sunrise Science Products). For growth resumption from stationary phase, logarithmically grown precultures were diluted to 0.5 A_{600nm}-units/ml and grown overnight to reach stationary phase. The cells were harvested by centrifugation and diluted into fresh medium to A_{600nm} of 0.3 (for growth analysis) or 1 (for lipid analyses). Where indicated, cerulenin was added to cultures from a 10 mg/ml stock solution in ethanol to a final concentration of 10 μg/ml. For lipidomics analysis, the cells were grown in SC medium containing 2% glucose.

Lipid Analysis and TAG Degradation In Vivo

Lipids were extracted according to Folch et al. (1957). In brief, equal amounts of cells were centrifuged, washed once in ice-cold water, resuspended in 330 μl of methanol and disrupted for 10 min by vortex mixing with glass beads. Six hundred and sixty microliters of chloroform was added and the samples were centrifuged for 10 min at 10,000 × g to remove debris. The organic solvent supernatant was recovered and washed once with 0.9% NaCl. The lower chloroform phase was dried under a stream of nitrogen and the lipids were resuspended in 20 μl chloroform and separated by thin-layer chromatography (TLC) on Silica60 plates using as a solvent petroleum/diethyl ether/glacial acetic acid (80/20/1.5 v/v/v). For the analysis of TAG levels in Figures 1C, 3A, and 3B, the cells were grown to stationary phase, collected by centrifugation, and resuspended in fresh medium to 1 A_{600nm}-units/ml. At the indicated time points, 10 A_{600nm}-units of cells were processed as described above. Lipids were visualized on TLC plates by staining the plates with iodine vapor. They were identified by comparison with lipid standards. The plates were scanned and the lipid species were quantified using ImageJ. The linearity of iodine staining in the range observed in the experiments was confirmed by analysis of TAG standard curves (Figure S1B). For analyzing TAG degradation in vivo (Figures S3B, S3C, S6D, and S6E), cells were grown to stationary phase in the presence of [1,2-^{14}C]-acetic acid (0.1 μCi/ml; PerkinElmer). After harvesting, the cells were resuspended in fresh, unlabeled medium to 1 A_{600nm}-unit/ml. At the indicated time points, 5 A_{600nm}-units of cells were processed as described above. Labeled lipids were visualized using a phosphoimager (Bio-Rad, PMI) and quantified using ImageJ. To analyze the re-esterification of DAG during growth resumption, the cells were grown to stationary phase and diluted into fresh medium containing 10 μg/ml cerulenin and [1-^{14}C]-palmitic acid (0.1 μCi/ml; PerkinElmer) or [1-^{14}C]-oleic acid (0.1 μCi/ml; PerkinElmer) to 1 A_{600nm}-unit/ml. At the indicated time points, 5 A_{600nm}-units of cells were processed as described above.

Fluorescence Microscopy

For fluorescence microscopy, yeast cells expressing the indicated GFP- or RFP-tagged proteins were grown in SC medium containing 2% glucose to stationary phase. Where indicated, the cells were diluted into fresh medium in the presence or absence of 10 μg/ml cerulenin. The cells were collected by centrifugation and washed once with PBS buffer before imaging. For staining of lipid droplets, aliquots of cells were incubated with BODIPY 493/503 (final concentration 1 μg/ml) for 15 min at 30°C. The cells were washed twice with PBS before imaging. For the quantification of lipid droplets per cell, ten randomly chosen microscopy images of BODIPY-stained wild-type (WT) or ice2Δ cells were analyzed. The number of BODIPY 493/503 stained lipid droplets per cells in each image was determined using the CellProfiler software.

COS7 cells were transfected using 1 μg DNA of plasmid and the transfection reagent Lipofectamine (Invitrogen). The cells were incubated for 12 hr at 37°C in Dulbecco's modified Eagle's medium, 10% fetal bovine serum, and 1 mM sodium pyruvate in the presence of 5% CO_2. For immunofluorescence and fluorescence microscopy, the cells were trypsinized, transferred onto acid-washed glass coverslips, and incubated for 24 hr in a 12-well tissue culture dish (BD Biosciences). The cells were fixed by replacing the medium with PBS containing 4% paraformaldehyde and incubated for 20–30 min at room temperature. They were washed with PBS and permeabilized by incubation for 10 min in PBS containing 0.1% Triton X-100 (Thermo Scientific). Immunocytochemistry was carried out by incubating the permeabilized cells with antibodies against calreticulin, diluted in PBS containing 1% calf serum (Gibco). The cells were washed three times in PBS and then incubated with AlexaFluor-labeled secondary antibodies and 0.1 μg/ml BODIPY 493 (Invitrogen).

Images were acquired using a Nikon Ti motorized inverted microscope equipped with 100× Plan Apo N 1.4 objective lens, a Hamamatsu ORCA-R2 cooled charge-coupled device (CCD) camera, and Metamorph 7 software. Alternatively (Figures 7D and S5C), images were captured using a Nikon TE2000U inverted microscope with a 100× Plan Apo NA 1.4 objective lens, a Hamamatsu ORCA ER cooled CCD camera, and MetaMorph software. The images were processed using Adobe Photoshop CS3.

Lipidome Analysis by Mass Spectrometry

Samples for the lipidome analysis in Figures 2B and S2A were harvested from cultures of yeast growing exponentially in SC medium containing 2% glucose, washed once in water at 4°C, and frozen in liquid nitrogen. Samples for analysis in Figures 4 and S3A were harvested at different time points after diluting stationary phase cells into fresh medium containing 10 μg/ml cerulenin and processed as described above. Lipid analysis was performed using a Triversa NanoMate ion source (Advion Biosciences) and a LTQ Orbitrap XL mass spectrometer (Thermo Fisher Scientific), as previously described (Ejsing et al., 2009).

Statistical Analysis

Quantitative data are presented as mean ± SD of three independent experiments. Results in Figures 4 and S3A are from two independent experiments, analyzed in duplicates, and presented as mean ± SD.

SUPPLEMENTAL INFORMATION

Supplemental Information includes Supplemental Experimental Procedures, six figures, and three tables and can be found with this article online at http://dx.doi.org/10.1016/j.celrep.2013.11.046.

ACKNOWLEDGMENTS

We thank the Nikon Imaging center at Harvard Medical School for help, Albert Casanovas for constructive discussions, and Pedro Carvalho for critically reading the manuscript. C.S.E. is supported by Lundbeckfonden (R44-A4342 and R54-A5858) and the Danish Council for Independent Research/Natural Sciences (09-072484). T.A.R. is a Howard Hughes Medical Institute investigator.

Received: October 15, 2013
Revised: November 1, 2013
Accepted: November 27, 2013
Published: December 26, 2013

REFERENCES

Adeyo, O., Horn, P.J., Lee, S., Binns, D.D., Chandrahas, A., Chapman, K.D., and Goodman, J.M. (2011). The yeast lipin orthologue Pah1p is important for biogenesis of lipid droplets. J. Cell Biol. *192*, 1043–1055.

Athenstaedt, K., and Daum, G. (2003). YMR313c/TGL3 encodes a novel triacylglycerol lipase located in lipid particles of Saccharomyces cerevisiae. J. Biol. Chem. *278*, 23317–23323.

Athenstaedt, K., and Daum, G. (2005). Tgl4p and Tgl5p, two triacylglycerol lipases of the yeast Saccharomyces cerevisiae are localized to lipid particles. J. Biol. Chem. *280*, 37301–37309.

Athenstaedt, K., Zweytick, D., Jandrositz, A., Kohlwein, S.D., and Daum, G. (1999). Identification and characterization of major lipid particle proteins of the yeast Saccharomyces cerevisiae. J. Bacteriol. *181*, 6441–6448.

Bickel, P.E., Tansey, J.T., and Welte, M.A. (2009). PAT proteins, an ancient family of lipid droplet proteins that regulate cellular lipid stores. Biochim. Biophys. Acta *1791*, 419–440.

Brasaemle, D.L. (2007). Thematic review series: adipocyte biology. The perilipin family of structural lipid droplet proteins: stabilization of lipid droplets and control of lipolysis. J. Lipid Res. *48*, 2547–2559.

Bulankina, A.V., Deggerich, A., Wenzel, D., Mutenda, K., Wittmann, J.G., Rudolph, M.G., Burger, K.N., and Höning, S. (2009). TIP47 functions in the biogenesis of lipid droplets. J. Cell Biol. *185*, 641–655.

Choudhary, V., Jacquier, N., and Schneiter, R. (2011). The topology of the triacylglycerol synthesizing enzyme Lro1 indicates that neutral lipids can be produced within the luminal compartment of the endoplasmatic reticulum: Implications for the biogenesis of lipid droplets. Commun. Integr. Biol. *4*, 781–784.

Costanzo, M., Baryshnikova, A., Bellay, J., Kim, Y., Spear, E.D., Sevier, C.S., Ding, H., Koh, J.L., Toufighi, K., Mostafavi, S., et al. (2010). The genetic landscape of a cell. Science *327*, 425–431.

Czabany, T., Athenstaedt, K., and Daum, G. (2007). Synthesis, storage and degradation of neutral lipids in yeast. Biochim. Biophys. Acta *1771*, 299–309.

Duncan, R.E., Ahmadian, M., Jaworski, K., Sarkadi-Nagy, E., and Sul, H.S. (2007). Regulation of lipolysis in adipocytes. Annu. Rev. Nutr. *27*, 79–101.

Eichmann, T.O., Kumari, M., Haas, J.T., Farese, R.V., Jr., Zimmermann, R., Lass, A., and Zechner, R. (2012). Studies on the substrate and stereo/regioselectivity of adipose triglyceride lipase, hormone-sensitive lipase, and diacylglycerol-O-acyltransferases. J. Biol. Chem. *287*, 41446–41457.

Ejsing, C.S., Sampaio, J.L., Surendranath, V., Duchoslav, E., Ekroos, K., Klemm, R.W., Simons, K., and Shevchenko, A. (2009). Global analysis of the yeast lipidome by quantitative shotgun mass spectrometry. Proc. Natl. Acad. Sci. USA *106*, 2136–2141.

Estrada de Martin, P., Du, Y., Novick, P., and Ferro-Novick, S. (2005). Ice2p is important for the distribution and structure of the cortical ER network in Saccharomyces cerevisiae. J. Cell Sci. *118*, 65–77.

Fakas, S., Konstantinou, C., and Carman, G.M. (2011). DGK1-encoded diacylglycerol kinase activity is required for phospholipid synthesis during growth resumption from stationary phase in Saccharomyces cerevisiae. J. Biol. Chem. *286*, 1464–1474.

Folch, J., Lees, M., and Sloane Stanley, G.H. (1957). A simple method for the isolation and purification of total lipides from animal tissues. J. Biol. Chem. *226*, 497–509.

Fujimoto, T., and Parton, R.G. (2011). Not just fat: the structure and function of the lipid droplet. Cold Spring Harb. Perspect. Biol. *3*, 3.

Garbarino, J., Padamsee, M., Wilcox, L., Oelkers, P.M., D'Ambrosio, D., Ruggles, K.V., Ramsey, N., Jabado, O., Turkish, A., and Sturley, S.L. (2009). Sterol and diacylglycerol acyltransferase deficiency triggers fatty acid-mediated cell death. J. Biol. Chem. *284*, 30994–31005.

Greenberg, A.S., Coleman, R.A., Kraemer, F.B., McManaman, J.L., Obin, M.S., Puri, V., Yan, Q.W., Miyoshi, H., and Mashek, D.G. (2011). The role of lipid droplets in metabolic disease in rodents and humans. J. Clin. Invest. *121*, 2102–2110.

Grillitsch, K., Connerth, M., Köfeler, H., Arrey, T.N., Rietschel, B., Wagner, B., Karas, M., and Daum, G. (2011). Lipid particles/droplets of the yeast Saccharomyces cerevisiae revisited: lipidome meets proteome. Biochim. Biophys. Acta *1811*, 1165–1176.

Han, S.H., Han, G.S., Iwanyshyn, W.M., and Carman, G.M. (2005). Regulation of the PIS1-encoded phosphatidylinositol synthase in Saccharomyces cerevisiae by zinc. J. Biol. Chem. *280*, 29017–29024.

Han, G.S., O'Hara, L., Siniossoglou, S., and Carman, G.M. (2008). Characterization of the yeast DGK1-encoded CTP-dependent diacylglycerol kinase. J. Biol. Chem. *283*, 20443–20453.

Henry, S.A., Kohlwein, S.D., and Carman, G.M. (2012). Metabolism and regulation of glycerolipids in the yeast Saccharomyces cerevisiae. Genetics *190*, 317–349.

Hickenbottom, S.J., Kimmel, A.R., Londos, C., and Hurley, J.H. (2004). Structure of a lipid droplet protein; the PAT family member TIP47. Structure *12*, 1199–1207.

Inokoshi, J., Tomoda, H., Hashimoto, H., Watanabe, A., Takeshima, H., and Omura, S. (1994). Cerulenin-resistant mutants of Saccharomyces cerevisiae with an altered fatty acid synthase gene. Mol. Gen. Genet. *244*, 90–96.

Jacquier, N., Choudhary, V., Mari, M., Toulmay, A., Reggiori, F., and Schneiter, R. (2011). Lipid droplets are functionally connected to the endoplasmic reticulum in Saccharomyces cerevisiae. J. Cell Sci. *124*, 2424–2437.

Kagiwada, S., Hosaka, K., Murata, M., Nikawa, J., and Takatsuki, A. (1998). The Saccharomyces cerevisiae SCS2 gene product, a homolog of a synaptobrevin-associated protein, is an integral membrane protein of the endoplasmic reticulum and is required for inositol metabolism. J. Bacteriol. *180*, 1700–1708.

Koh, J.L., Ding, H., Costanzo, M., Baryshnikova, A., Toufighi, K., Bader, G.D., Myers, C.L., Andrews, B.J., and Boone, C. (2010). DRYGIN: a database of quantitative genetic interaction networks in yeast. Nucleic Acids Res. *38* (Database issue), D502–D507.

Krahmer, N., Guo, Y., Wilfling, F., Hilger, M., Lingrell, S., Heger, K., Newman, H.W., Schmidt-Supprian, M., Vance, D.E., Mann, M., et al. (2011). Phosphatidylcholine synthesis for lipid droplet expansion is mediated by localized activation of CTP:phosphocholine cytidylyltransferase. Cell Metab. *14*, 504–515.

Kuchler, K., Daum, G., and Paltauf, F. (1986). Subcellular and submitochondrial localization of phospholipid-synthesizing enzymes in Saccharomyces cerevisiae. J. Bacteriol. *165*, 901–910.

Kuerschner, L., Moessinger, C., and Thiele, C. (2008). Imaging of lipid biosynthesis: how a neutral lipid enters lipid droplets. Traffic *9*, 338–352.

Kurat, C.F., Natter, K., Petschnigg, J., Wolinski, H., Scheuringer, K., Scholz, H., Zimmermann, R., Leber, R., Zechner, R., and Kohlwein, S.D. (2006). Obese yeast: triglyceride lipolysis is functionally conserved from mammals to yeast. J. Biol. Chem. *281*, 491–500.

Kurat, C.F., Wolinski, H., Petschnigg, J., Kaluarachchi, S., Andrews, B., Natter, K., and Kohlwein, S.D. (2009). Cdk1/Cdc28-dependent activation of the major triacylglycerol lipase Tgl4 in yeast links lipolysis to cell-cycle progression. Mol. Cell *33*, 53–63.

Lankester, D.L., Brown, A.M., and Zammit, V.A. (1998). Use of cytosolic triacylglycerol hydrolysis products and of exogenous fatty acid for the synthesis of triacylglycerol secreted by cultured rat hepatocytes. J. Lipid Res. *39*, 1889–1895.

Leber, R., Zinser, E., Zellnig, G., Paltauf, F., and Daum, G. (1994). Characterization of lipid particles of the yeast, Saccharomyces cerevisiae. Yeast *10*, 1421–1428.

Listenberger, L.L., Han, X., Lewis, S.E., Cases, S., Farese, R.V., Jr., Ory, D.S., and Schaffer, J.E. (2003). Triglyceride accumulation protects against fatty acid-induced lipotoxicity. Proc. Natl. Acad. Sci. USA *100*, 3077–3082.

Loewen, C.J., and Levine, T.P. (2005). A highly conserved binding site in vesicle-associated membrane protein-associated protein (VAP) for the FFAT motif of lipid-binding proteins. J. Biol. Chem. *280*, 14097–14104.

Loewen, C.J., Young, B.P., Tavassoli, S., and Levine, T.P. (2007). Inheritance of cortical ER in yeast is required for normal septin organization. J. Cell Biol. *179*, 467–483.

Longtine, M.S., McKenzie, A., 3rd, Demarini, D.J., Shah, N.G., Wach, A., Brachat, A., Philippsen, P., and Pringle, J.R. (1998). Additional modules for versatile and economical PCR-based gene deletion and modification in Saccharomyces cerevisiae. Yeast *14*, 953–961.

Murphy, S., Martin, S., and Parton, R.G. (2009). Lipid droplet-organelle interactions; sharing the fats. Biochim. Biophys. Acta *1791*, 441–447.

Natter, K., Leitner, P., Faschinger, A., Wolinski, H., McCraith, S., Fields, S., and Kohlwein, S.D. (2005). The spatial organization of lipid synthesis in the yeast Saccharomyces cerevisiae derived from large scale green fluorescent protein tagging and high resolution microscopy. Mol. Cell. Proteomics *4*, 662–672.

North, M., Steffen, J., Loguinov, A.V., Zimmerman, G.R., Vulpe, C.D., and Eide, D.J. (2012). Genome-wide functional profiling identifies genes and processes important for zinc-limited growth of Saccharomyces cerevisiae. PLoS Genet. *8*, e1002699.

Oelkers, P., Tinkelenberg, A., Erdeniz, N., Cromley, D., Billheimer, J.T., and Sturley, S.L. (2000). A lecithin cholesterol acyltransferase-like gene mediates diacylglycerol esterification in yeast. J. Biol. Chem. *275*, 15609–15612.

Oelkers, P., Cromley, D., Padamsee, M., Billheimer, J.T., and Sturley, S.L. (2002). The DGA1 gene determines a second triglyceride synthetic pathway in yeast. J. Biol. Chem. *277*, 8877–8881.

Penno, A., Hackenbroich, G., and Thiele, C. (2013). Phospholipids and lipid droplets. Biochim. Biophys. Acta *1831*, 589–594.

Petschnigg, J., Wolinski, H., Kolb, D., Zellnig, G., Kurat, C.F., Natter, K., and Kohlwein, S.D. (2009). Good fat, essential cellular requirements for triacylglycerol synthesis to maintain membrane homeostasis in yeast. J. Biol. Chem. *284*, 30981–30993.

Rajakumari, S., Rajasekharan, R., and Daum, G. (2010). Triacylglycerol lipolysis is linked to sphingolipid and phospholipid metabolism of the yeast Saccharomyces cerevisiae. Biochim. Biophys. Acta *1801*, 1314–1322.

Rasmussen, J.T., Faergeman, N.J., Kristiansen, K., and Knudsen, J. (1994). Acyl-CoA-binding protein (ACBP) can mediate intermembrane acyl-CoA transport and donate acyl-CoA for beta-oxidation and glycerolipid synthesis. Biochem. J. *299*, 165–170.

Raussens, V., Fisher, C.A., Goormaghtigh, E., Ryan, R.O., and Ruysschaert, J.M. (1998). The low density lipoprotein receptor active conformation of apolipoprotein E. Helix organization in n-terminal domain-phospholipid disc particles. J. Biol. Chem. *273*, 25825–25830.

Sandager, L., Gustavsson, M.H., Ståhl, U., Dahlqvist, A., Wiberg, E., Banas, A., Lenman, M., Ronne, H., and Stymne, S. (2002). Storage lipid synthesis is nonessential in yeast. J. Biol. Chem. *277*, 6478–6482.

Schuldiner, M., Collins, S.R., Thompson, N.J., Denic, V., Bhamidipati, A., Punna, T., Ihmels, J., Andrews, B., Boone, C., Greenblatt, J.F., et al. (2005). Exploration of the function and organization of the yeast early secretory pathway through an epistatic miniarray profile. Cell *123*, 507–519.

Sorger, D., and Daum, G. (2002). Synthesis of triacylglycerols by the acyl-coenzyme A:diacyl-glycerol acyltransferase Dga1p in lipid particles of the yeast Saccharomyces cerevisiae. J. Bacteriol. *184*, 519–524.

Soto-Cardalda, A., Fakas, S., Pascual, F., Choi, H.S., and Carman, G.M. (2012). Phosphatidate phosphatase plays role in zinc-mediated regulation of phospholipid synthesis in yeast. J. Biol. Chem. *287*, 968–977.

Stone, S.J., Levin, M.C., and Farese, R.V., Jr. (2006). Membrane topology and identification of key functional amino acid residues of murine acyl-CoA:diacylglycerol acyltransferase-2. J. Biol. Chem. *281*, 40273–40282.

Szymanski, K.M., Binns, D., Bartz, R., Grishin, N.V., Li, W.P., Agarwal, A.K., Garg, A., Anderson, R.G., and Goodman, J.M. (2007). The lipodystrophy protein seipin is found at endoplasmic reticulum lipid droplet junctions and is important for droplet morphology. Proc. Natl. Acad. Sci. USA *104*, 20890–20895.

Tavassoli, S., Chao, J.T., Young, B.P., Cox, R.C., Prinz, W.A., de Kroon, A.I., and Loewen, C.J. (2013). Plasma membrane—endoplasmic reticulum contact sites regulate phosphatidylcholine synthesis. EMBO Rep. *14*, 434–440.

Walther, T.C., and Farese, R.V., Jr. (2012). Lipid droplets and cellular lipid metabolism. Annu. Rev. Biochem. *81*, 687–714.

Wang, C.W., and Lee, S.C. (2012). The ubiquitin-like (UBX)-domain-containing protein Ubx2/Ubxd8 regulates lipid droplet homeostasis. J. Cell Sci. *125*, 2930–2939.

Wiggins, D., and Gibbons, G.F. (1992). The lipolysis/esterification cycle of hepatic triacylglycerol. Its role in the secretion of very-low-density lipoprotein and its response to hormones and sulphonylureas. Biochem. J. *284*, 457–462.

Wilfling, F., Wang, H., Haas, J.T., Krahmer, N., Gould, T.J., Uchida, A., Cheng, J.X., Graham, M., Christiano, R., Fröhlich, F., et al. (2013). Triacylglycerol synthesis enzymes mediate lipid droplet growth by relocalizing from the ER to lipid droplets. Dev. Cell *24*, 384–399.

Wilson, C., Wardell, M.R., Weisgraber, K.H., Mahley, R.W., and Agard, D.A. (1991). Three-dimensional structure of the LDL receptor-binding domain of human apolipoprotein E. Science *252*, 1817–1822.

Wolinski, H., Kolb, D., Hermann, S., Koning, R.I., and Kohlwein, S.D. (2011). A role for seipin in lipid droplet dynamics and inheritance in yeast. J. Cell Sci. *124*, 3894–3904.

Yang, L.Y., Kuksis, A., Myher, J.J., and Steiner, G. (1995). Origin of triacylglycerol moiety of plasma very low density lipoproteins in the rat: structural studies. J. Lipid Res. *36*, 125–136.

Zanghellini, J., Natter, K., Jungreuthmayer, C., Thalhammer, A., Kurat, C.F., Gogg-Fassolter, G., Kohlwein, S.D., and von Grünberg, H.H. (2008). Quantitative modeling of triacylglycerol homeostasis in yeast—metabolic requirement for lipolysis to promote membrane lipid synthesis and cellular growth. FEBS J. *275*, 5552–5563.

Zechner, R., Kienesberger, P.C., Haemmerle, G., Zimmermann, R., and Lass, A. (2009). Adipose triglyceride lipase and the lipolytic catabolism of cellular fat stores. J. Lipid Res. *50*, 3–21.

Supplemental Information

Extended Experimental Procedures

Yeast Strains and Plasmid Construction

Gene deletion and tagging was done by homologous recombination of PCR fragments. Ice2p, Erg6p and Tgl3p were genomically tagged at the N-terminus using a GFP-HIS3 cassette amplified from pFA6a-GFP-HIS3 (Longtine et al., 1998). N-terminal genomic tagging of Erg6p with RFP was done by using a RFP-KanMX cassette amplified from pFA6a-mRFP-KanMX6 (Huh et al., 2003). A deletion of *ice2* was generated using a PCR fragment containing the URA3 marker and flanking regions of the *ice2* gene, amplified from plasmid pRS316. To generate plasmids carrying C-terminal GFP tagged versions of Ice2p, Ice2p amino acids 241-357 (Ice2(cyt)), and Dga1p, GFP was amplified from pFA6a-GFP-KanMX, digested with XhoI/HindIII and ligated into XhoI/HindIII sites of p415-ADHpr (Nguyen et al., 2012). Ice2p and Ice2p aa241-357 (Ice2(cyt)) were amplified from genomic DNA and, after digestion with XbaI / SmaI, they were ligated into the XbaI/SmaI sites of p415-ADHpr-GFP. Dga1p was amplified from genomic DNA and ligated into XbaI/HindII sites of p415-ADHpr-GFP after digestion. To generate a plasmid carrying C-terminal mRFP-tagged Dga1p, the plasmid encoding Dga1-GFP was digested with HindIII / XhoI, to replace GFP with PCR-amplified and HindIII / XhoI-digested mRFP. To generate a plasmid encoding a C-terminal GFP-tagged version of Ice2p, lacking the cytoplasmic loop (aa241-357, ∆cyt), Ice2∆cyt was generated by fusion of two PCR products, Ice2 1-241 and Ice2 357-492. The resulting PCR product was digested with SmaI / XbaI and ligated into SmaI / XbaI sites of p415-ADHpr-GFP. For expression of an RFP tagged version of Ice2p aa241-357 (Ice2(cyt)) in COS7 cells, Ice2 aa241-357 was amplified from genomic DNA and, after digestion with SalI /SacII, ligated into the SalI/SacII site of pAcRFP-C1.

In vitro phosphatidylserine conversion assay

To measure the conversion of PS to PE in vitro (Figure S2B), yeast cells were grown at 30°C to early-logarithmic phase in SC medium containing 2% Glucose. Crude mitochondria (containing ER-mitochondrial contact sites) were purified as previously described (Daum et al., 1982). One hundred µL crude mitochondria (100 µg protein) in 0.6 m mannitol, 20 mm Tris pH 7.4 and 0.6 mm $MnCl_2$ were incubated with 0.1 µCi L-[^{14}C(U)]-serine at 30°C. After 20 min, 40 mM unlabeled serine was added, and PS synthesis was arrested by addition of 5 mM EDTA. The conversion of PS to PE was then followed during a 45 min incubation period at 30°C. The reaction was stopped by adding 1 mL chloroform:methanol 2:1 (v/v). After shaking for 1 h, lipids were extracted, the organic phase was washed with 100 µL 0.9% NaCl (w/v), and dried at 65°C. Lipids were resuspended in 15 µL chloroform, separated on thin-layer chromatography plates (Silica 60) in chloroform/methanol/25% ammonium hydroxide (50/25/6 v/v/v). They were visualized using a phosphoimager (BioRad, PMI). Radioactive lipids were quantified using ImageJ software. Data reported are the mean +/- SD for three experiments.

Table S1: Yeast strains used in this study

Strain ID	Genotype	Source
BY4741	*MAT**a** his3Δ1 leu2Δ0 met15Δ0 ura3Δ0*	(Brachmann et al., 1998)
YDM104	*MAT**a*** his3Δ1 leu2Δ0 met15Δ0 ura3Δ0 ICE2::KanMX	Open Biosystems
YDM194	*MAT**a*** his3Δ1 leu2Δ0 met15Δ0 ura3Δ0 ICE2::GFP-HIS3	This study
YDM218	*MAT**a*** his3Δ1 leu2Δ0 met15Δ0 ura3Δ0 TGL3::GFP-HIS3	This study
YDM222	*MAT**a*** his3Δ1 leu2Δ0 met15Δ0 ura3Δ0 ICE2::KanMX TGL3::GFP-HIS3	This study
YDM260	*MAT**a*** his3Δ1 leu2Δ0 met15Δ0 ura3Δ0 ERG6::GFP-HIS3	This study
YDM261	*MAT**a*** his3Δ1 leu2Δ0 met15Δ0 ura3Δ0 ICE2::KanMX ERG6::GFP-HIS3	This study
YDM316	*MAT**a*** his3Δ1 leu2Δ0 met15Δ0 ura3Δ0 ERG6::RFP-KanMX	This study
YDM320	*MAT**a*** his3Δ1 leu2Δ0 met15Δ0 ura3Δ0 ERG6::RFP-KanMX ICE2::GFP-HIS3	This study
YDM383	*MAT**a*** his3Δ1 leu2Δ0 met15Δ0 ura3Δ0 TGL3::KanMX	Open Biosystems
YDM388	*MAT**a*** his3Δ1 leu2Δ0 met15Δ0 ura3Δ0 DGA1::KanMX	Open Biosystems
YDM397	*MAT**a*** his3Δ1 leu2Δ0 met15Δ0 ura3Δ0 TGL3::KanMX ICE2::GFP-HIS3	This study
YDM415	*MAT**a*** his3Δ1 leu2Δ0 met15Δ0 ura3Δ0 DGA1::KanMX ICE2::URA3	This study

Table S2: Plasmids used in this study

ID	Name	Reference
158	p415-ADHpr-Ice2-GFP	This study
185	p415-ADHpr-Dga1-GFP	This study
193	p415-ADHpr-Ice2 (aa241-357)-GFP	This study
189	pAcRFP-C1-Ice2 aa241-357	This study
210	p415-ADHpr-Dga1-mRFP	This study
224	p415-ADHpr-Ice2Δcyt-GFP	This study

Table S3: Genetic interactions of Ice2; selected, from DRYGIN Database

Negative genetic interactions	Positive genetic interactions
Dgk1, Scs2, Ino2, Scs3, Psd2, Ino4, Cho2, Opi3, Psd1, Are2, Pct1, Erg12, Sct1 (Gat2), Ect1, CKI1	Fld1, Scs7, Pah1, Erg6, Erg3, Erg25

References

Brachmann, C.B., Davies, A., Cost, G.J., Caputo, E., Li, J., Hieter, P., and Boeke, J.D. (1998). Designer deletion strains derived from Saccharomyces cerevisiae S288C: a useful set of strains and plasmids for PCR-mediated gene disruption and other applications. Yeast 14, 115-132.

Daum, G., Gasser, S.M., and Schatz, G. (1982). Import of proteins into mitochondria. Energy-dependent, two-step processing of the intermembrane space enzyme cytochrome b2 by isolated yeast mitochondria. The Journal of biological chemistry 257, 13075-13080.

Huh, W.K., Falvo, J.V., Gerke, L.C., Carroll, A.S., Howson, R.W., Weissman, J.S., and O'Shea, E.K. (2003). Global analysis of protein localization in budding yeast. Nature 425, 686-691.

Koh, J.L., Ding, H., Costanzo, M., Baryshnikova, A., Toufighi, K., Bader, G.D., Myers, C.L., Andrews, B.J., and Boone, C. (2010). DRYGIN: a database of quantitative genetic interaction networks in yeast. Nucleic acids research 38, D502-507.

Longtine, M.S., McKenzie, A., 3rd, Demarini, D.J., Shah, N.G., Wach, A., Brachat, A., Philippsen, P., and Pringle, J.R. (1998). Additional modules for versatile and economical PCR-based gene deletion and modification in Saccharomyces cerevisiae. Yeast 14, 953-961.

Nguyen, T.T., Lewandowska, A., Choi, J.Y., Markgraf, D.F., Junker, M., Bilgin, M., Ejsing, C.S., Voelker, D.R., Rapoport, T.A., and Shaw, J.M. (2012). Gem1 and ERMES do not directly affect phosphatidylserine transport from ER to mitochondria or mitochondrial inheritance. Traffic 13, 880-890.

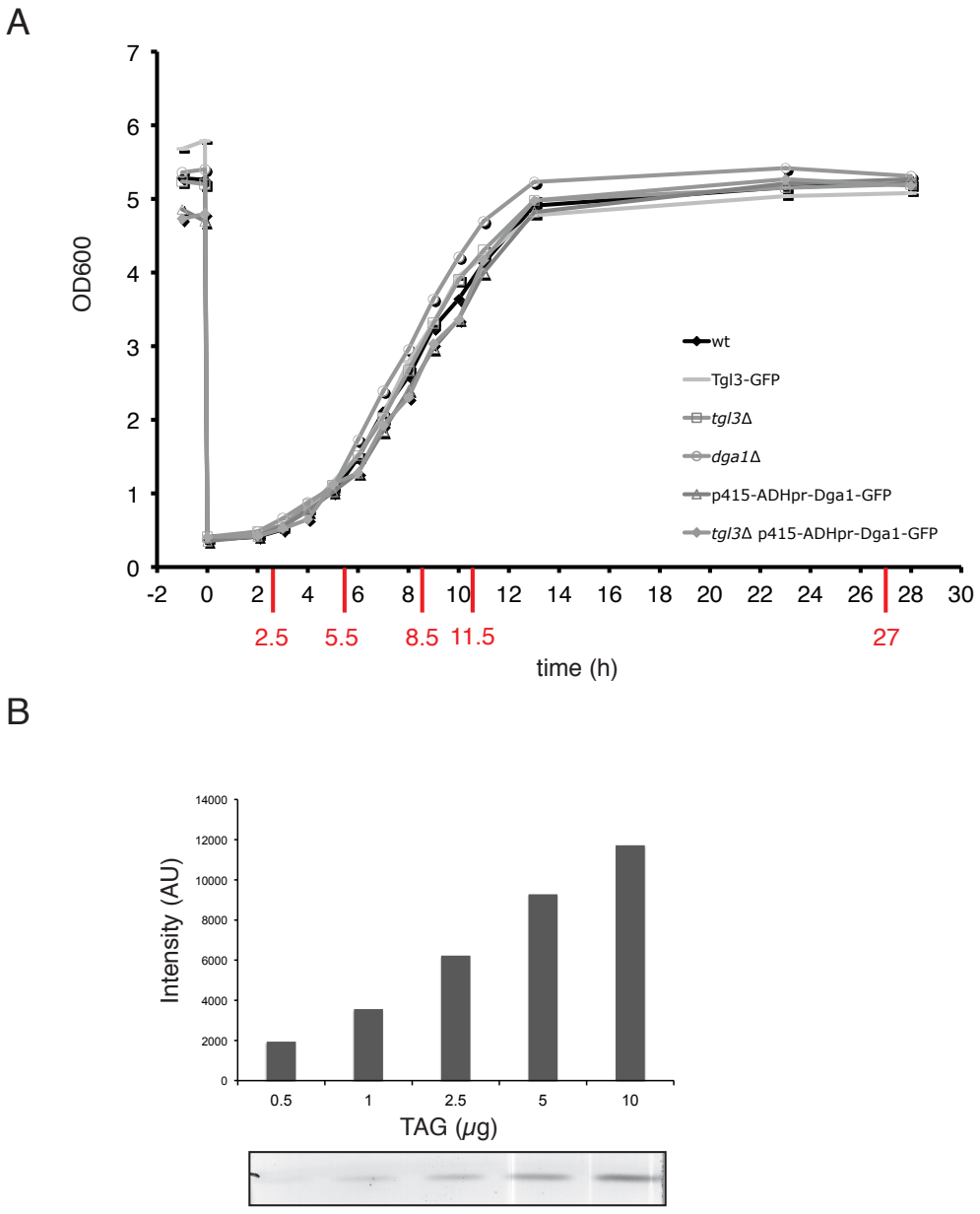

Figure S1. Time-points analyzed during the growth of different yeast strains and validation of TAG analysis by iodine staining, related to Figure 1.

(A) Wild type (WT) and the indicated mutant cells were diluted from stationary phase into fresh medium and their growth was followed by measuring the OD at 600nm. Samples, analyzed in Figure 1, were taken at the time points labeled in red. (B) The linearity of the TAG assay was verified by separating the indicated amounts of TAG by TLC, followed by iodine staining. TLC plates were scanned and quantified using ImageJ.

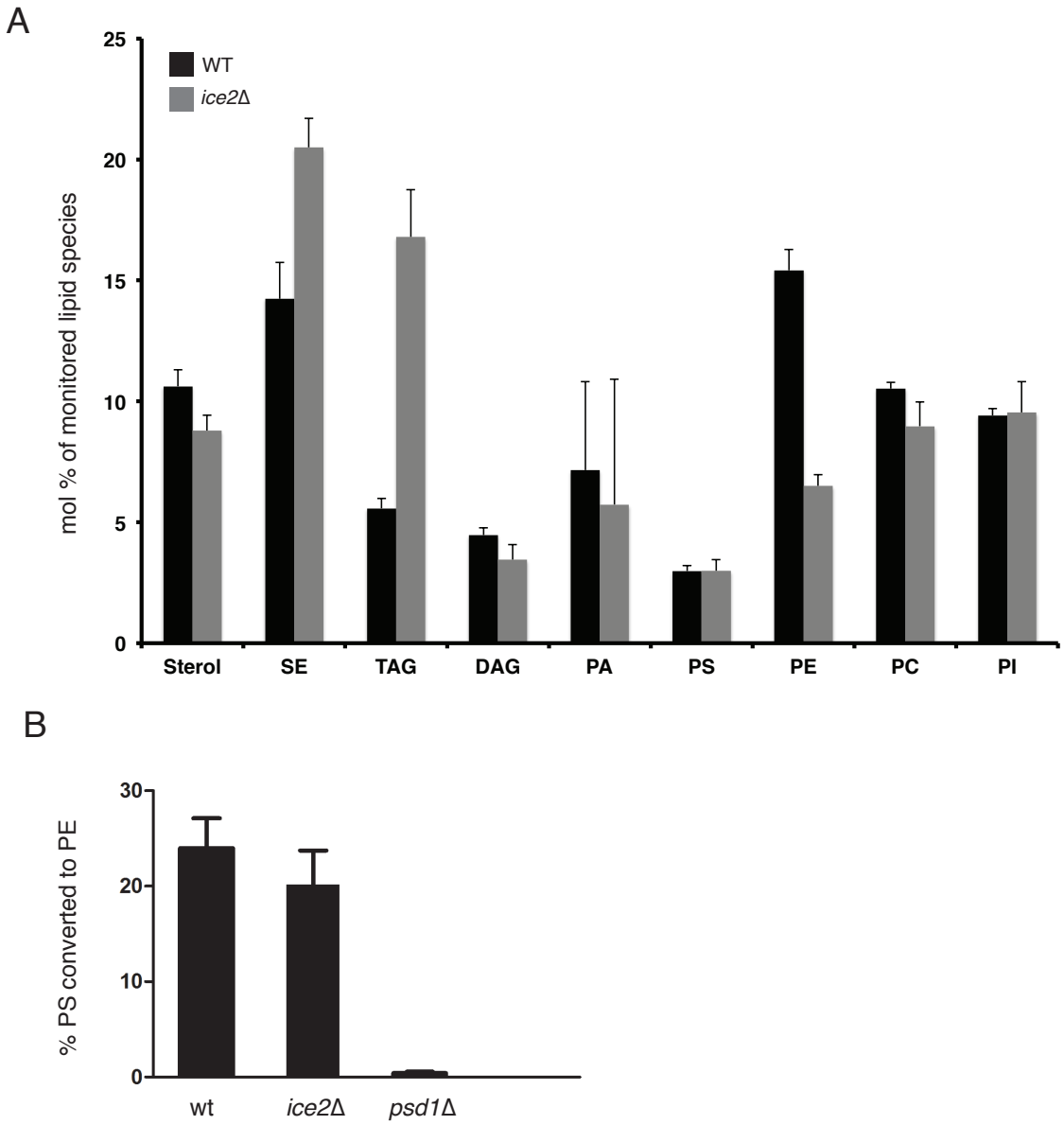

Figure S2. Ice2p affects phospholipid levels independently of mitochondrial decarboxylation of PE, related to Figure 3.

(A) Lipid composition of WT and *ice2*Δ cells, harvested at 0.6 A_{600nm}-unit/ml, were determined after lipid extraction and analysis by quantitative mass spectrometry. Data from three independent experiments are shown as mean +/- SD. (B) The conversion of PS to PE was determined *in vitro* using crude mitochondria incubated with radioactive serine. The percentage of radiolabeled PS converted to PE in WT and mutant mitochondria is shown. Bars and error bars represent the mean +/- SD from three independent experiments.

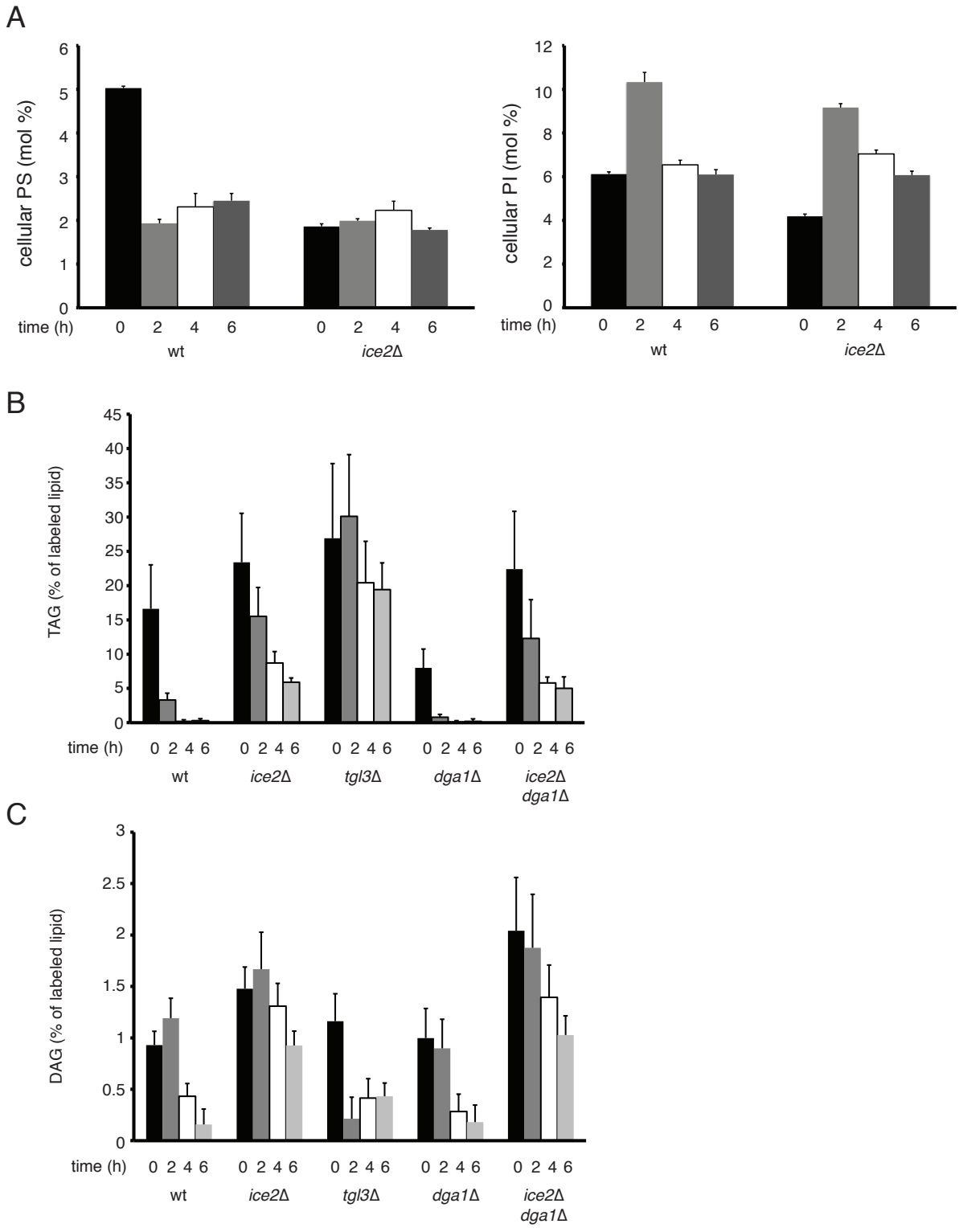
A
cellular PS (mol %)
cellular PI (mol %)
time (h)
0 2 4 6
wt
ice2Δ
B
TAG (% of labeled lipid)
wt
ice2Δ
tgl3Δ
dga1Δ
ice2Δ dga1Δ
C
DAG (% of labeled lipid)

Figure S3. Lipid composition and DAG accumulation during growth resumption in cells lacking Ice2p, related to Figure 4.

(A) The lipid composition of wild type (WT) and *ice2*Δ cells was analyzed after dilution of cells from stationary phase into fresh medium containing 10 µg/ml cerulenin. Samples were taken at different time points after dilution and PS and PI were analyzed by quantitative mass spectrometry. Data from two independent experiments, analyzed in duplicates, are shown as mean +/- SD. (B) Wild type (WT) cells and the indicated mutants were grown to stationary phase in the presence of ^{14}C-acetic acid and diluted into fresh medium containing 10 µg/ml cerulenin. The levels of labeled TAG were determined at different time points by TLC, followed by phosphorimaging and analysis by ImageJ. Labeled TAG was normalized to the total radioactivity in the chloroform-extracted fraction. Data from three independent experiments are shown as mean +/- SD. (C) As in (B), but labeled DAG was analyzed.

A

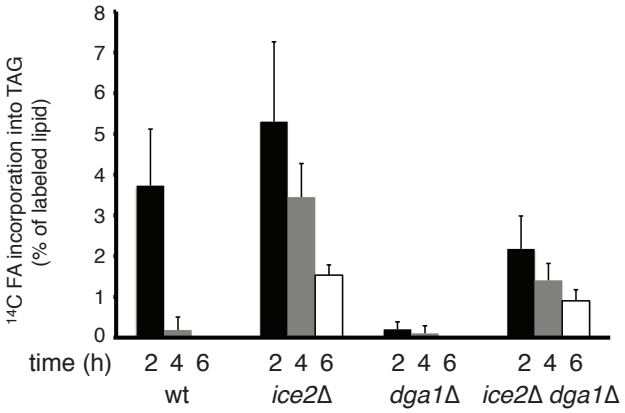

B

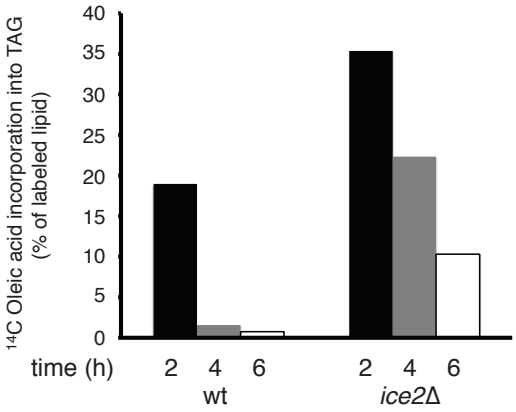

Figure S4. The re-esterification of DAG to TAG is dependent on Dga1p, related to Figure 5.

(A) The incorporation of ^{14}C-palmitic acid into TAG was determined for wild type (WT), and the indicated mutant cells at different time points after dilution from stationary phase into fresh medium containing 10µg/ml cerulenin and ^{14}C-palmitic acid. The lipids were separated by TLC and quantitated by phosphorimaging and analysis by ImageJ. TAG levels were normalized to the total radioactivity in the chloroform-extracted fraction. and are presented as mean +/- SD of four independent expriments. (B) As in (A), but with ^{14}C-oleic acid.

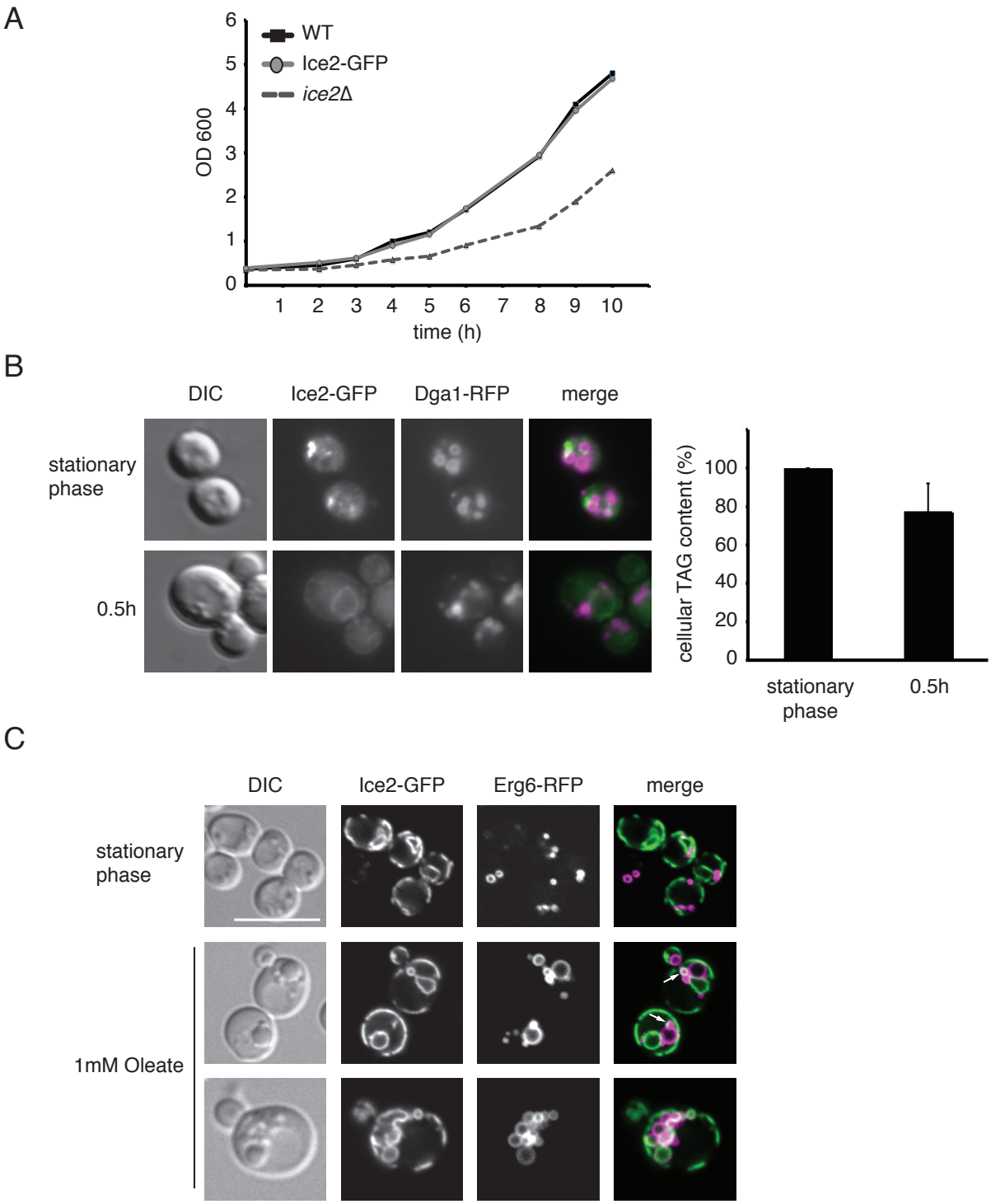
A
WT
Ice2-GFP
ice2Δ
OD 600
time (h)
B
DIC
Ice2-GFP
Dga1-RFP
merge
stationary phase
0.5h
cellular TAG content (%)
stationary phase
0.5h
C
DIC
Ice2-GFP
Erg6-RFP
merge
stationary phase
1mM Oleate

Figure S5. Re-localization of Ice2p-GFP, related to Figure 6.

(A) Wild type (WT) cells, *ice2*Δ cells, or cells in which the endogenous ICE2 gene was replaced by a GFP-tagged version, were diluted from stationary phase into fresh medium and their growth was followed by measuring the OD at 600nm. (B) The localization of Ice2-GFP was analyzed by fluorescence microscopy at stationary phase and 0.5h after dilution into fresh medium. The cells also expressed Dga1-mRFP from a plasmid as a marker for LDs. The graph shows TAG levels at stationary phase and 30min after dilution into fresh medium. Lipids were extracted at the indicated time points and analyzed by TLC followed by iodine staining and quantification using ImageJ. (C) The localization of Ice2p-GFP, overexpressed from a plasmid, was analyzed by fluorescence microscopy at stationary phase and 6h after dilution into fresh medium containing 1 mM oleate. The cells also expressed Erg6p-RFP as a marker for LDs. Arrows indicate Ice2-GFP positive structures in contact with Erg6-RFP labeled LDs. Scale bar: 10 μm.

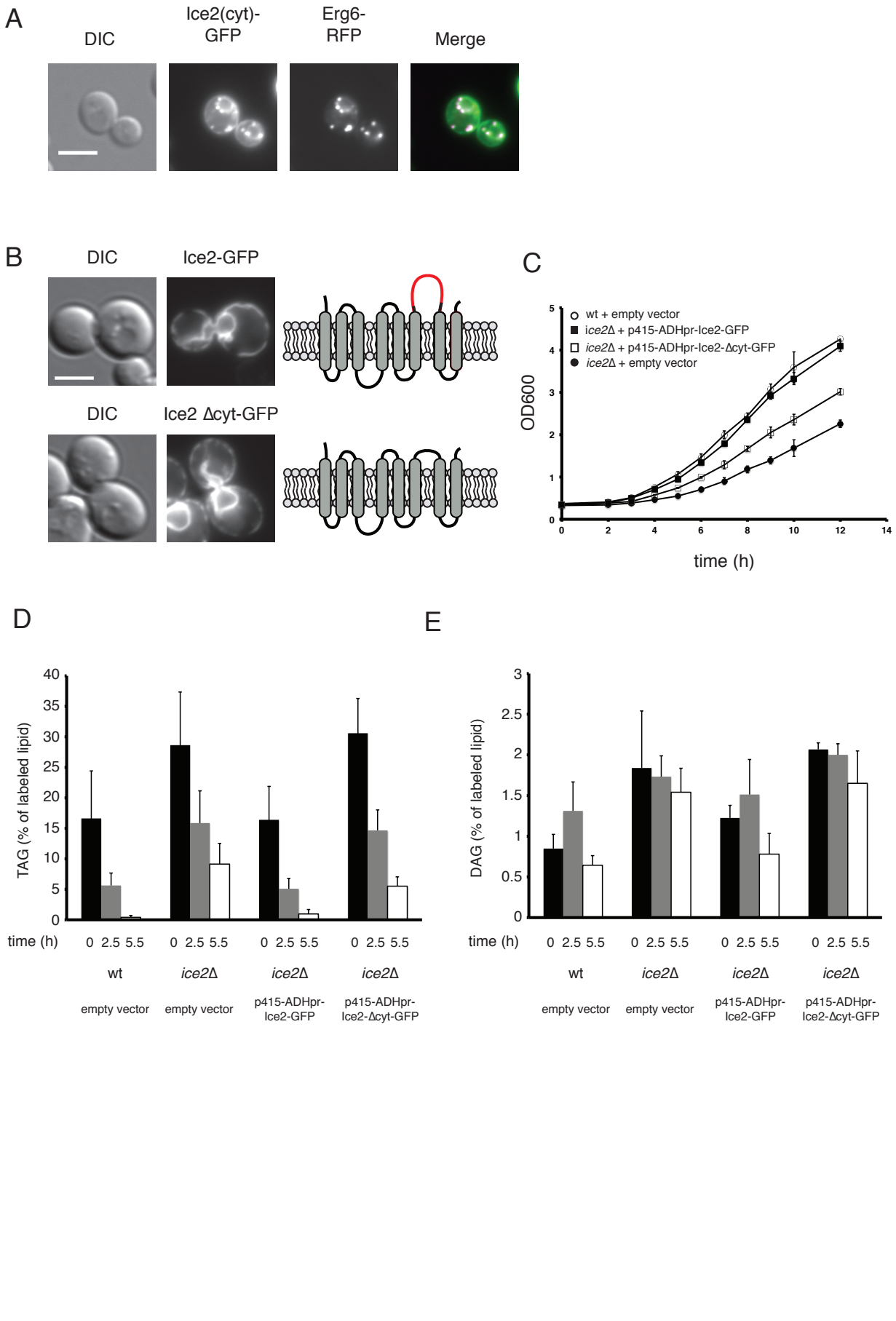
A
DIC
Ice2(cyt)-GFP
Erg6-RFP
Merge
B
DIC
Ice2-GFP
DIC
Ice2 Δcyt-GFP
C
wt + empty vector
ice2Δ + p415-ADHpr-Ice2-GFP
ice2Δ + p415-ADHpr-Ice2-Δcyt-GFP
ice2Δ + empty vector
OD600
time (h)
D
TAG (% of labeled lipid)
time (h)
0 2.5 5.5
wt
empty vector
ice2Δ
empty vector
ice2Δ
p415-ADHpr-Ice2-GFP
ice2Δ
p415-ADHpr-Ice2-Δcyt-GFP
E
DAG (% of labeled lipid)
time (h)
0 2.5 5.5
wt
empty vector
ice2Δ
empty vector
ice2Δ
p415-ADHpr-Ice2-GFP
ice2Δ
p415-ADHpr-Ice2-Δcyt-GFP

Figure S6 (related to Figure 7). A cytoplasmic domain of Ice2p interacts with LDs and is required for Ice2p function.

(A) The localization of the cytoplasmic loop of Ice2p (Ice2(cyt)-GFP),expressed from a plasmid, was analyzed by fluorescence microscopy in exponentially growing cells. The cells also expressed Erg6-RFP as a marker for LDs. Scale bar: 5 µm. (B) *ice2*Δ mutant cells overexpressing Ice2-GFP or Ice2 Δcyt-GFP from a plasmid were analyzed by fluorescence microscopy in exponentially growing cells. (C) Growth of wild type cells or *ice2*Δ cells overexpressing Ice2p-GFP or Ice2 Δcyt-GFP from a plasmid under the ADH promoter. (D) Wild type (WT) and *ice2*Δ mutant cells carrying the indicated plasmids were grown to stationary phase in the presence of ^{14}C-acetic acid and diluted into fresh medium containing 10 µg/ml cerulenin. The levels of labeled TAG were determined at different time points by TLC, followed by phosphorimaging and analysis by ImageJ. Labeled TAG was normalized to the total radioactivity in the chloroform-extracted fraction. Data from three independent experiments are shown as mean +/- SD. (E) As in (D), but labeled DAG was analyzed.